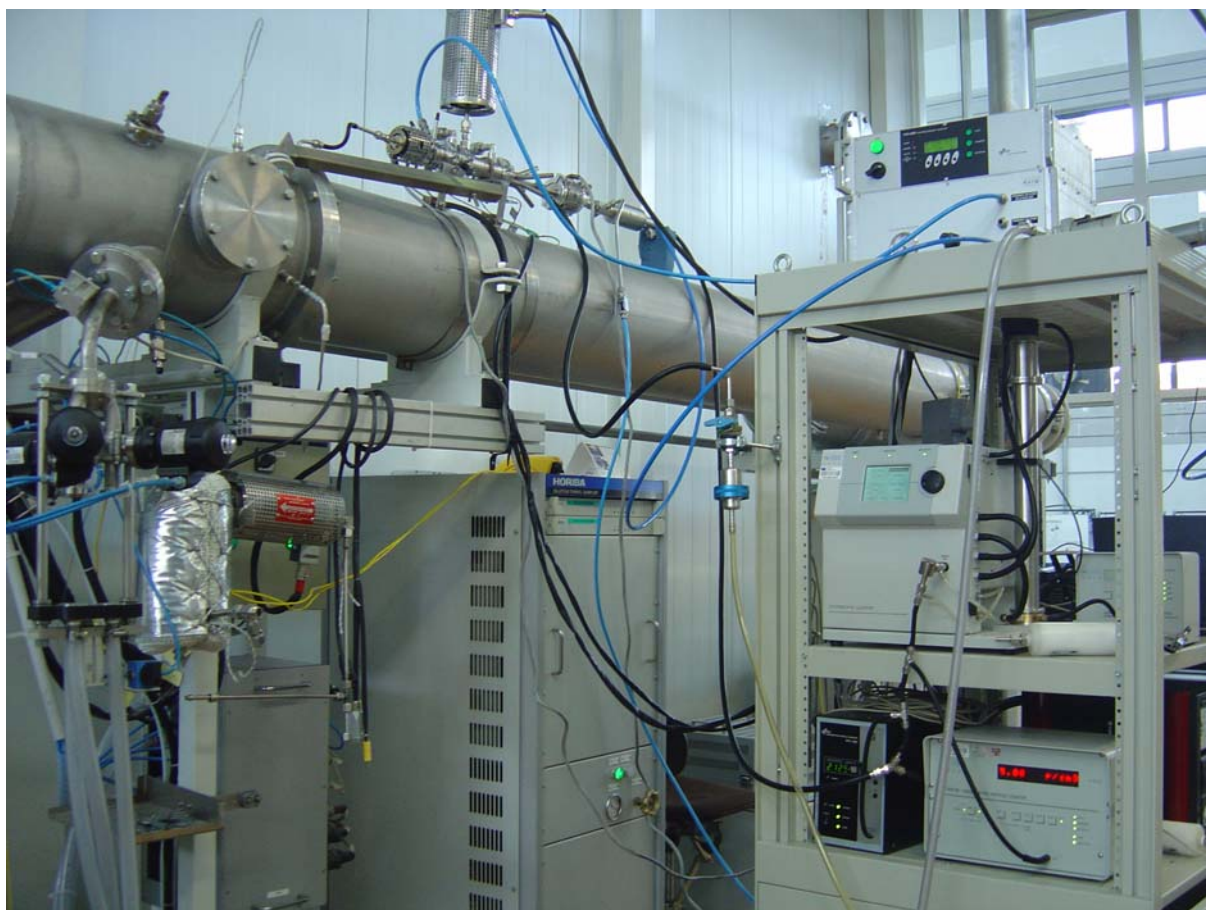


Measurements in support of modelling the VELA-2 experimental facilities

Barouch Giechaskiel, Lorenzo Isella, Rinaldo Colombo, Urbano Manfredi,
Panagiota Dilara, Yannis Drossinos, Alois Krasenbrink, Giovani De Santi



EUR 23043 EN - 2007

The mission of the Institute for Environment and Sustainability is to provide scientific-technical support to the European Union's Policies for the protection and sustainable development of the European and global environment.

European Commission
Joint Research Centre
Institute for Environment and Sustainability

Contact information

Yannis Drossinos (T.P. 441)
Address: Transport and Air Quality Unit, Institute for Environment and Sustainability,
Joint Research Centre, Via E. Fermi, I-21027 Ispra (VA), Italy
E-mail: ioannis.drossinos@jrc.it
Tel.: +39 0332 78 5387
Fax: +39 0332 78 5236

<http://ies.jrc.ec.europa.eu>
<http://www.jrc.ec.europa.eu>

Legal Notice

Neither the European Commission nor any person acting on behalf of the Commission is responsible for the use which might be made of this publication.

***Europe Direct is a service to help you find answers
to your questions about the European Union***

**Freephone number (*):
00 800 6 7 8 9 10 11**

(*) Certain mobile telephone operators do not allow access to 00 800 numbers or these calls may be billed

A great deal of additional information on the European Union is available on the Internet.
It can be accessed through the Europa server <http://europa.eu/>

JRC 41981

EUR 23043 EN
ISBN 978-92-79-07146-1
ISSN 1018-5593
DOI 10.2788/55159

Luxembourg: Office for Official Publications of the European Communities

© European Communities, 2007

Reproduction is authorised provided the source is acknowledged

Printed in Italy

Contents

1. INTRODUCTION	1
2. EXPERIMENTAL METHOD	3
TEST VEHICLE.....	3
FUEL.....	4
SAMPLING SYSTEMS AND CONDITIONS.....	4
Dilution air	5
Exhaust gas transfer tube (Anaconda).....	5
Dilution tunnel	5
Sampling positions	5
Temperature profile measurements	5
Particle sampling.....	6
Instrumentation	7
LOSSES	8
PM SAMPLING.....	9
GASEOUS POLLUTANTS	9
STEADY-STATE TESTS	9
TEST PROTOCOL	9
3. RESULTS	14
Test protocol.....	14
Stability	16
Repeatability	16
Wet – dry measurements (Cold – Hot dilution)	17
Effect of sampling position.....	19
Mixing point	24
Temperature profiles.....	24
Comparison of instruments	27
ANNEXES	33
A. FPS and Ejector dilutors.....	33
B. DMM	36
C. SMPS and CPCs.....	37
D. Temperature profiles at 50 km/h.....	41
Temperature profiles over time	41
Radial temperature profiles	43
E. Temperature profiles at 120 km/h.....	46
Temperature profiles over time	46
Radial temperature profiles	48

List of Figures

Figure 1: The vehicle used for the measurements was a FIAT Stilo (Euro 3).	3
Figure 2: Measurement points of particle and temperature profiles. Details in the text.	4
Figure 3: Particle number sampling set up. Abbreviations explained at the end of the document.	6
Figure 4: Examples of measurement at a) sampling position b) end of anaconda and c) tailpipe.	11
Figure 5: Typical measurement: temperature data.	14
Figure 6: Typical measurement: particle instruments data.	15
Figure 7: Results of the measurements of the previous Figure for the Mass, CPC (3025A) and SMPS. The Mass is calculated from the weight on the filter corrected for the dilution ratio (DR), CVS flow-rate, and vehicle speed. SMPS is the average of the 3 scans corrected for FPS DR and the CVS DR. CPC is the average from the times that the 3 SMPS scans were taken (corrected for the FPS DR and the CVS DR).	15
Figure 8: Stability of SMPS size distribution results.	16
Figure 9: Repeatability of measurements at 120 km/h a) at CVS b) at the end of anaconda.	17
Figure 10: Comparison of wet and dry measurement for 50 km/h at different sampling positions (always in the middle of the tube).	18
Figure 11: Comparison of wet and dry measurement for 120 km/h at different sampling positions (always in the middle of the tube).	18
Figure 12: Size distributions at different sampling positions (middle of tube) for 50 km/h.	19
Figure 13: Size distributions at different sampling positions (middle of tube) for 120 km/h	20
Figure 14: Concentration and mean diameter at different sampling positions at 50 km/h.	22
Figure 15: Concentration and mean diameter at different sampling positions at 120 km/h.	22
Figure 16: Mass results at different sampling positions for the case of 50 km/h.	23
Figure 17: Mass results at different sampling positions for the case of 120 km/h.	23
Figure 18: Size distributions at the end of anaconda and at different radial positions at the mixing position at CVS. Percentages show the necessary CVS correction at the mixing point to match the “inlet” (end anaconda) size distribution.	25
Figure 19: Size distributions at the end of anaconda and at different radial positions at the mixing position at CVS. Percentages show the necessary CVS correction at the mixing point to match the “inlet” (end anaconda) size distribution. CVS flow rate a) 6 and b) 12 m ³ /min.	26
Figure 20: Correlation between the two CPCs used in the study.	27
Figure 21: Correlation between TSI’s CPC and SMPS.	28
Figure 22: Correlation between DEKATI’s CPC and TSI’s SMPS.	28
Figure 23: Correlation between DMM and SMPS.	29
Figure 24: Correlation between DMM and filter measurements. There is a poor correlation with the FPS mass results due to the low mass collected on the filters. There is a very good correlation with the CVS results.	29

List of Tables

Table 1: Vehicle relevant characteristics	3
Table 2: Specifications of dilution air system	5
Table 3: Sampling positions for particle and temperature measurements. At column “Reps” the number on the left of the slash indicates the number of repetitions for particle (radial) profiles measurements and the number on the right indicates repetitions for temperature (radial) profiles measurements.	6
Table 4: Temperature (radial) profile position measurements	6
Table 5: Estimation of losses due to diffusion at the sampling lines. No thermophoresis is taken into account.	8
Table 6: Procedure of filter heating in the furnace (N ₂ atmosphere).	9
Table 7: Regulated gaseous emissions measurement equipment.	9
Table 8: Measurements for the modeling of VELA-2 facilities. 3T indicates temperature profile measurements (radial).	12
Table 9: Summary of SMPS results for 50 km/h and 120 km/h	21

Acknowledgments

The authors would like to gratefully acknowledge Dekati Ltd. for kindly providing the sampling system, the mass monitor and the particle number counter. We would like to thank Philippe Le Lijour and Gaston Lanappe for their excellent hard work and the long hours they spent in the laboratory during the tests.

1. INTRODUCTION

Diesel exhaust fine particles are extensively studied, both experimentally and theoretically, because they have been associated with various effects, ranging from adverse health effect to climate change. Current European regulations for light-duty diesel engine particle emissions are based on total emitted particulate mass. The exhaust gases of vehicles are diluted in a (full) dilution tunnel from where a sample is drawn and collected on a filter. Recent research results suggest, however, that different metrics, such as number distribution or active surface, may quantify particles effect more precisely, especially their possible health-related.

There are also concerns about how representative the results from the dilution tunnel are compared to the emissions at the tailpipe. Maricq et al. (1999) showed that there are differences between tailpipe and dilution tunnel in mass and number. Although they emphasized mainly the differences in the nucleation mode of the size distribution, the figures in their study show that there are also differences in the accumulation mode (in figure 10 in their paper the size distribution at the tunnel is narrower, at bigger diameters and with lower concentration). Vogt and Scheer (2002) presented that the size distributions at the tailpipe and the dilution tunnel were different with similar tendency as the one described by Maricq et al. (1999). They attributed the differences to coagulation. More recently Casati et al (2007) found even bigger differences between the tailpipe and the dilution tunnel size distributions. The studies mentioned before measured total particles (volatile and non-volatile part) as their sampling systems used dilution air at ambient temperature, so many phenomena could explain the differences they observed (e.g. nucleation, condensation, agglomeration, deposition etc). There is a drawback with their approach: by favouring procedures like nucleation and condensation at the tailpipe measurements, the effect of the sampling system cannot be isolated from the procedures that take place actually in the transfer tube. Simple calculations show that no nucleation and condensation takes place in the transfer tube and in order to study the procedures that take place the sampling conditions must be such that only the accumulation (soot) mode is measured. In this direction the "PMP" protocol is more appropriate.

The Particulate Measurement Programme (PMP), an international collaborative programme, has been established to develop a measurement protocol to measure repeatably (small intra-laboratory variation) and reproducibly (inter-laboratory variation) particle number emissions to replace, or complement, the existing mass-based system for regulatory purposes. According to PMP the particle number system should consist of a first stage hot dilution at 150°C and dilution ration of at least 10:1 and then a heated section at 300-400°C for the removal of volatiles, avoiding thus the uncertainty of the volatiles which affects the repeatability (and reproducibility) of the measurements. A second dilution to cool down the diluted sample is also recommended. However, in order to minimize required changes to the current type approval facilities, the system will be sampling from the full dilution tunnel. The results of the light duty phase of the PMP, which were recently published (Andersson et al. 2007), showed that the number method has better sensitivity than the mass method and can be used for legislative purposes. In fact a new number limit of 5×10^{11} is already proposed (Good 2007). There are general guidelines for the sampling point at the dilution tunnel (10-20 diameters downstream the mixing point) and the transfer tube (<6.1 m and <10.5 cm inner diameter). However there are significant differences in the lengths of the transfer tubes between the laboratories. For example, in the studies of Ntziachristos et al. (2005) and Vogt and Scheer (2002) 6 m insulated tubes were used, in the study of Maricq and Xu (2004) a 8 m (10 cm inner diameter) was used and the laboratory of the present study has 9 m heated line.

It is, thus, essential to investigate particle dynamics in the transfer tube from the tailpipe to the dilution tunnel, to ensure that measurements in different laboratories are comparable and to suggest the most appropriate experimental geometry for regulatory measurements. This document reports the results of measurements conducted at the VELA-2 laboratories of the JRC in February 2007. The aim of the experimental campaign was to provide the necessary experimental data to model aerosol processes from the vehicle's exhaust tailpipe to the sampling point at the full dilution tunnel. The measurements included particle and temperature profiles at the tailpipe, at the end of the exhaust gas transfer tube to the dilution tunnel (anaconda), at the diaphragm of the dilution tunnel, 1,5 tunnel diameters downstream the diaphragm and 10 tunnel diameters downstream the diaphragm (normal sampling point). Two steady state speeds were used (50 and 120 km/h) and flow rates at the dilution tunnel of 6 and 12 m³/min. Non-volatile and total particle number and mass concentrations were measured according to the protocol of the Particulate Measurement Programme.

The results showed that the main changes of particle number distributions are observed along the transfer tube from the tailpipe to the dilution tunnel (anaconda). Afterwards the particle number distributions remain almost constant. However, low dilution at the dilution tunnel (flow rate of 6 m³/min) leads to a further small particle number distribution change.

2. EXPERIMENTAL METHOD

In the following sections the experimental details for the measurements conducted in the JRC VELA-2 facilities will be described. Details in Giechaskiel et al. (2007b).

TEST VEHICLE

The vehicle used in this study (Figure 1) was a FIAT Stilo JTD (Euro 3). The mileage of the vehicle at the beginning of the experiments was 71911 km. Information can be seen in Table 1.

Table 1: Vehicle relevant characteristics

Vehicle	Diesel FIAT Stilo JTD
Engine type	1.9 JTD
Capacity (cc)	1910
Cylinder number / Valves per cylinder	4 / 2
Max. Power (kW @ rpm)	85 @ 4000
Max. Torque (Nm @ rpm)	280 @ 2000
Combustion concept	Common rail D.I.
Aspiration	Turbocharged
Vehicle Inertia (kg)	1365
Emission Standard	98/68/EC (Euro3 without DPF)
Consumption (l/100 km) according to ECE 93/116	7,0 / 4,2 / 5,3 (urban, extra-urban, mixed)
CO2 93/116/CE (g/km)	144



Figure 1: The vehicle used for the measurements was a FIAT Stilo (Euro 3).

FUEL

The (market) fuel used in this vehicle had a sulfur content of less than 50 ppm.

SAMPLING SYSTEMS AND CONDITIONS

Sampling was conducted according to current legislation and the proposals of the Particle Measurement Programme (PMP). The measurements were done on a 48" 4x4 dynamometer MAHA SN 87 (roller diameter of 1.220 m and 150 kW) at the JRC laboratories. The general overview of the experimental set up can be seen in Figure 2. In the following paragraphs the figure will be explained in detail.

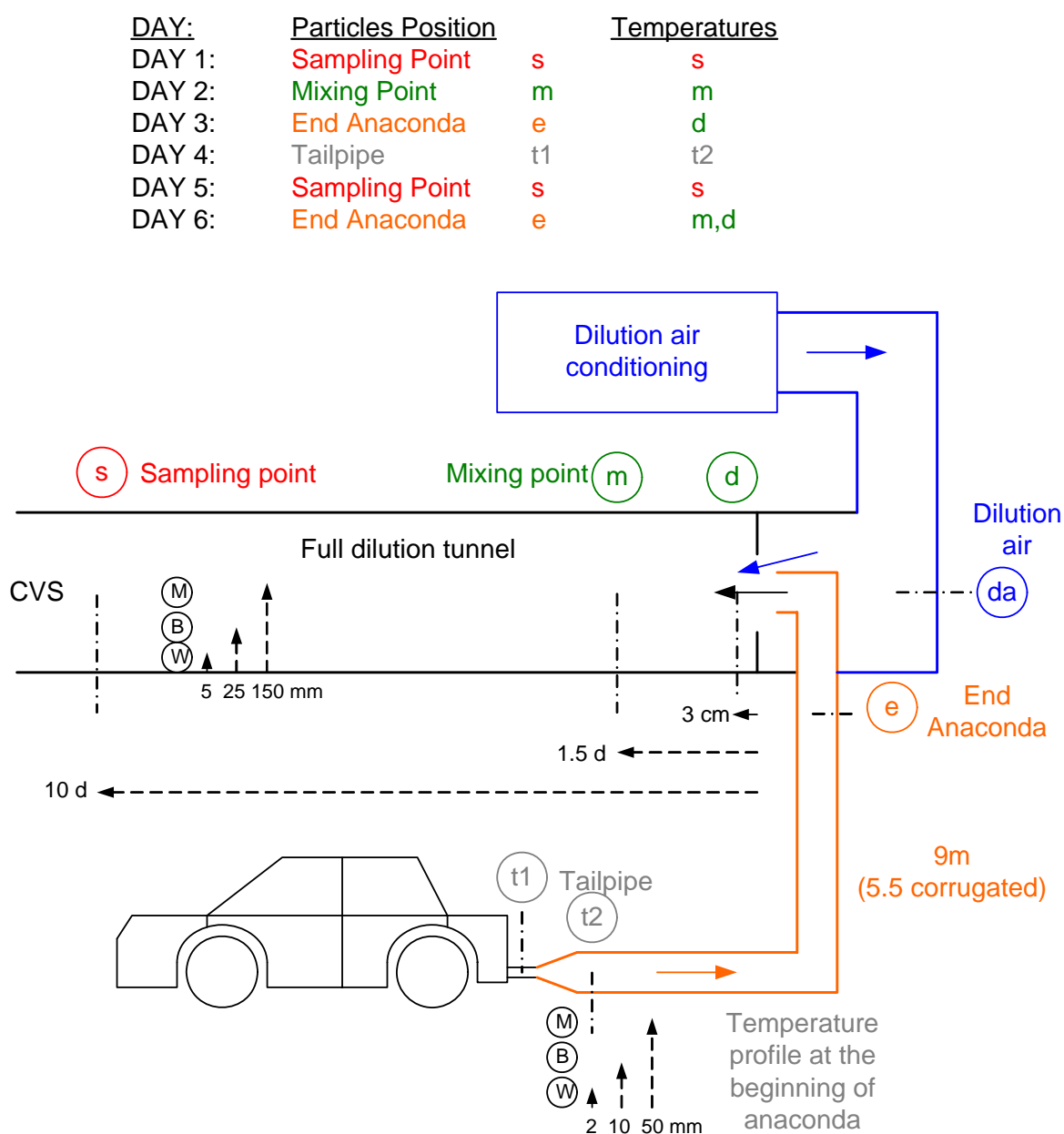


Figure 2: Measurement points of particle and temperature profiles. Details in the text.

Dilution air

The exhaust gas was primarily diluted and conditioned following the Constant Volume Sampling (CVS) procedure. Highly efficient dilution air filters for particles and hydrocarbons that reduce particle contributions from the dilution air to near zero were used (99.99% of reduction for particles with size diameter of 0.3 μm) (Table 2). The temperature of the dilution air and the relative humidity were conditioned to $23\pm 1^\circ\text{C}$ and $50\pm 5\%$ relative humidity. Particle measurements were taken at the dilution air line before any mixing with the exhaust gases (position da).

Table 2: Specifications of dilution air system

Type	Model	Efficiency	Flow [m^3/h]	ΔP [Pa]
Particle Filter	3QMHF242412-90	85/90-F7 CEN EN 779	2000	50
Active Charcoal	CAMCARB 1000-CM05		2000	40
Particle Filter	SOLIFAIR 1560.02	H13-N1822 : 99.99 @ 0.3 μm	2000	120

Exhaust gas transfer tube (Anaconda)

The vehicle was coupled to the CVS transfer line by a metal-to-metal join during testing to avoid the possibility of exhaust contamination by the high-temperature breakdown of elastomer coupling elements (position t1). The exhaust was transported to the tunnel through a 9 m long (10 cm inner diameter) stainless steel tube (the end of the tube is considered position e). The first 5.5 m of the tube were corrugated and heated at 70°C , while the rest 3.5 m were heated to 60°C . The exhaust was introduced to the full dilution tunnel along the tunnel axis, near an orifice plate that ensured rapid mixing with the dilution air (position d). Exhaust gas temperature (T_{exh}) was also measured at the end of tailpipe (position t1), approximately 25 cm before the beginning of anaconda (or position t2).

Dilution tunnel

The flow rate of dilute exhaust gas through the tunnel was controlled by a critical orifice venturi. Flow rates of approximately 6 or 12 m^3/min were used in the measurements. The tunnel operated in the turbulent flow regime ($\text{Re} = 21.000$ or 53.500). Based on standard reference flow rates, the mean dilution ratio achieved in the CVS was 6:1 or 12:1 at 50 km/h (3rd gear), and 2.8 or 5.6:1 at 120 km/h (5th gear). The residence time of the exhaust in the dilution tunnel till the normal sampling point (10 tunnel diameters downstream the mixing point, position s) was 2.6 or 1.3 s for 6 and 12 m^3/min respectively. Extra measurements were taken 1.5 tunnel diameters from the orifice plate (position m).

Sampling positions

In order to model the temperature and particle changes at the experimental configuration, temperature and particle concentrations were measured at different sampling positions (Figure 2 and Table 3):

Temperature profile measurements

Temperature measurements (in the center of the ducts) were always taken for all the sampling positions of Figure 2. Moreover, in order to get an idea of the temperature (radial) profile of the diluted exhaust gas, 3 thermocouples of different lengths were used (3T). Table 4 shows their positioning along the diameter of the dilution tunnel. These three thermocouples were used at the sampling point (position s), at the mixing point (position m) and at the diaphragm point (position d). Three other thermocouples were used for some measurements at the inlet of the transfer tube to CVS (anaconda, position t2). Their positioning along the diameter of the anaconda can also be seen in Figure 2.

Table 3: Sampling positions for particle and temperature measurements. At column “Reps” the number on the left of the slash indicates the number of repetitions for particle (radial) profiles measurements and the number on the right indicates repetitions for temperature (radial) profiles measurements.

	Sampling position	Comments	Reps
da	Dilution air	Dilution air before mixing with exhaust gas	1/10+
t1	Tailpipe	Exhaust gas before entering the anaconda	1/3
e	End anaconda	Exhaust gas at the end of anaconda	2/2
d	Diaphragm	3 cm downstream the diaphragm (orifice plate)	-/2
m	Mixing point	50 cm (1.5 tunnel diameters downstream the diaphragm)	1/4
s	Sampling point	Normal position 10 tunnel diameters downstream the diaphragm	2/5

Table 4: Temperature (radial) profile position measurements

	Position	CVS (diameter 30 cm)	Anaconda (inlet) (diameter 10 cm)
w	Walls	0.5 cm from the walls of the CVS	0.2 cm from the walls of the CVS
b	Between	2.5 cm from the walls of the CVS	1.0 cm from the walls of the CVS
m	Middle	15 cm from the walls of the CVS (in the center)	5.0 cm from the walls of the CVS (in the center)

Particle sampling

Aerosol samples for particle number measurements were drawn with a modified Fine Particle Sampler (FPS) (Dekati Ltd.) with short not heated sampling lines (Ntziachristos et al. 2005). The same length probes were used at all different sampling positions at the dilution tunnel (positions **s**, **m** and **d**).

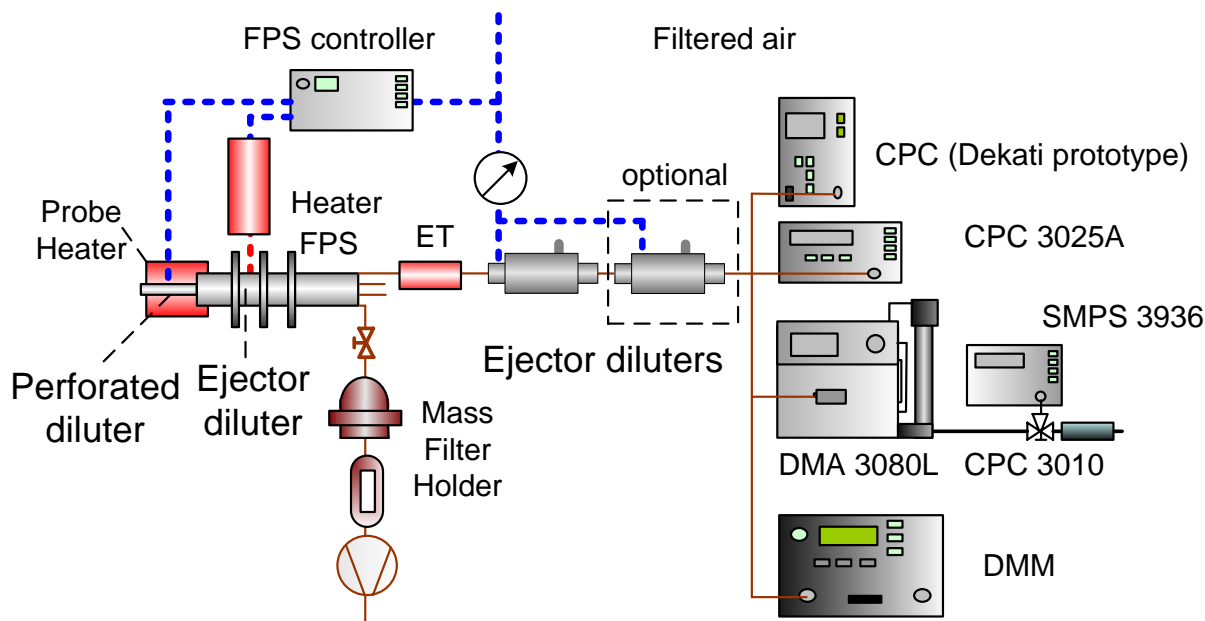


Figure 3: Particle number sampling set up. Abbreviations explained at the end of the document.

With FPS, dilution is carried out in two phases. The first dilution phase is conducted as close to a sampling point as possible, i.e., in a perforated tube diluter. This method assists reproducible results and prevents losses. The first, i.e., primary dilution can be hot or cold. With hot dilution condensation of volatile species can be prevented. With cold dilution the nucleation and condensation of volatile species can be maximized. The second dilution phase is an ejector type diluter, located downstream the primary dilution. The ejector diluter acts as a pump sucking a known amount of a diluted sample from the primary dilution. Simultaneously, a secondary dilution is carried out. In the FPS, critical parameters of the dilution are controlled and simultaneously monitored. Consequently, a sample is transformed from high temperature and high concentration to moderate levels in a controlled manner. The dilution ratio of the measurement can be calculated reliably, thus the measured concentration of particles can be converted to an actual particle concentration. With the controlled dilution temperature, a reliable 'wet' or 'dry' sample can be achieved and therefore the uncertainties in particle size are minimized. Details for principles of operation can be found in Appendix A.

In this study most measurements were according to the PMP protocol (hot dilution). The dilution ratios used were between 30:1 and 40:1 (probe diluter dilution ratio 1.5:1 to 2:1 and ejector diluter dilution ratio 17:1 to 20:1). The temperature was set to 400°C for the probe heater and 150°C for the (ejector) dilution air in order to evaporate volatile particles and reduce the partial pressures of the gas phase species to prevent re-condensation at the diluter exit. These temperatures led to diluted aerosol temperatures at the exit of the diluter ~120°C.

The temperature of the evaporation tube (ET) was set at 400°C in order to evaporate all volatiles and semi-volatile compounds. The residence time in this tube was estimated 0.15 s.

Some measurements were conducted without any heating at FPS in order to measure volatile particles also (as nucleation mode or condensed material on the soot particles). These measurements are noted as "cold" dilution measurements because ambient temperature air was used for the dilution. The particles measured with cold dilution are called "wet" particles in order to distinguish them from the normal measurements (PMP protocol or "hot" dilution that give as a result non-volatile or "dry" particles). Immediately downstream the evaporation tube there was an ejector diluter in order to cool the hot diluted exhaust gas, minimize the thermophoretic losses, and reduce the particle number concentration below 10^5 cm^{-3} in order to be within the detection limit of the CPCs. The dilution ratio was constant 10.5:1 for the specific overpressure (1 bar) in this set up (Giechaskiel et al. 2004). An extra ejector diluter was used in some measurements (e.g. tailpipe and end anaconda) where the particle number concentrations were higher. The dilution ratio of this diluter was calculated 13.5:1. The calculations of the dilution ratios were done with particle measurements upstream and downstream the diluters as no calibration gas or flow-meters were available at that period (Details in the xls file "DRs for CVS modeling") but as the ejectors have negligible losses the two values are almost the same (Ntziachristos et al. 2004). The ejector diluters were cleaned only at the beginning of the measurement campaign.

Instrumentation

Two CPCs (TSI Inc. 3025A, Dekati prototype), one SMPS (TSI Inc. 3936) and one DMM (Dekati Ltd.) were measuring total particle number concentration, particle number size distribution and mass concentration respectively downstream the ejector diluter. In this study sheath/sample flow rates used were 3/0.3 as it has been found that the 3936 neutralizer is not very efficient for higher flow rates. The flow rates were checked with a bubble flow-meter (BUCK calibrator M-5). The upscan and downscan times for the SMPS were 90/30 s respectively. More details about the instruments can be found in Annexes B and C.

Mass samples were drawn downstream the FPS with a flow rate of 30 lpm. A long metal tube was used to cool the hot (~120°C) diluted exhaust gas. The mass collected on the filters downstream FPS was in the order of 150 µg. The results of these filters will be shown but it must be emphasised that they were not taken into consideration as it was found later that the tygon tube that was used to connect the FPS to the filter holder created a “volatile” artifact for mass measurements (but no effect for number measurements).

LOSSES

Great care was taken to use identical lengths and flows for all measurements to make sure that the losses were the same for all cases. For this reason no correction for particle losses is made in the particle number results. An idea of the worst case scenario losses is seen in Table 5. These losses take into account gravitational settling, inertial deposition and diffusion losses (but not thermophoretic losses) inside the sampling system (FPS and tubes) (Hinds 1999, Baron & Willeke 2001). For the measured particle sizes gravitational settling and inertial deposition were minimal. As it can be seen the losses for particles in the size range of 50-100 nm (where the peak of the particle number size distribution lies) is in total less than 3% for all instruments. Losses for particles at 10 nm are high (up to 25%) but as there was no nucleation mode in the measurements these losses were of no importance.

The losses reported do not include possible thermophoretic losses. These losses will be similar for all cases as well. However when sampling from the tailpipe the thermophoretic losses from the tailpipe to the entrance of the sampling unit can be high.

Table 5: Estimation of losses due to diffusion at the sampling lines. No thermophoresis is taken into account.

Probe	Q [lpm]	L [cm]	d(in) [mm]	RT [s]	Flow	Losses		
						10 nm	50 nm	100 nm
Probe	5	30	5	0.07	laminar flow	2.0%	0.2%	0.1%
tygon	5	10	5	0.02	laminar flow	1.0%	0.1%	0.1%
FPS metal	5	15	5	0.04	laminar flow	1.3%	0.2%	0.1%
PM metal	30	55	10	0.09	turbulent flow	2.5%	0.3%	0.1%
PM tygon	30	60	8	0.06	turbulent flow	3.2%	0.4%	0.2%
PM holder	30	20	6	0.01	turbulent flow	0.5%	0.1%	0.0%
				0.29	Mass	10%	1%	1%
tygon	13.3	195	8	0.44	may be laminar or turbulent	12.1%	1.6%	0.7%
DMM tygon	10	55	8	0.17	laminar flow	1.9%	0.2%	0.1%
				0.74	DMM	18%	2%	1%
CPC DEKATI	3.3	5	5	0.02	laminar flow	0.8%	0.1%	0.0%
	1.5	30	5	0.24	laminar flow	4.3%	0.6%	0.2%
				0.82	CPC DEKATI	21%	3%	1%
CPC TSI	3.3	5	5	0.02	laminar flow	0.8%	0.1%	0.0%
	1.8	10	5	0.07	laminar flow	1.9%	0.2%	0.1%
	1.5	50	5	0.39	laminar flow	6.0%	0.8%	0.3%
				1.05	CPC TSI 3025A	25%	3%	1%
SMPS	3.3	5	5	0.02	laminar flow	0.8%	0.1%	0.0%
	1.8	10	5	0.07	laminar flow	1.9%	0.2%	0.1%
	0.3	10	5	0.39	laminar flow	6.0%	0.8%	0.3%
				1.05	SMPS TSI 3936	25%	3%	1%

PM SAMPLING

Mass samples were also drawn from the CVS at the normal sampling position (**position s**) at a constant flow rate of 25 lpm at normal conditions (0°C and 1 bar). Mass samples were collected on single 47 mm Quarzo filters to permit chemical analysis with a Sunset OC/EC analyser.

For some tests normal T60A20 filters were used at CVS. After their weight was determined the Non Volatile Fraction (NVF) content was determined indirectly with the following procedure: The previously loaded and weighted filters were heated (Table 6) in a furnace under continuous flux of N₂. Afterwards filters remained in the conditioning room for another 24 h and then heated filters weights were taken. NVF emissions of the vehicle were calculated as the difference between tare and heated filter weights. It should be noted that even when a blank filter follows this procedure losses some of it's mass (~30 µg for T60A20 filters) due to its volatile content. This weight loss was also taken into account, but it didn't affect the results as the weight of the filters at CVS was >1500 µg.

Table 6: Procedure of filter heating in the furnace (N₂ atmosphere)

Phase	Starting Temperature (°C)	Final Temperature (°C)	Duration (min)
1	ambient	150	30
2	150	300	120
3	300	220	120
4	220	100	60

GASEOUS POLLUTANTS

The gaseous emissions were measured in accordance with the current R83 regulation. A Horiba MEXA-7400HTR-LE instrument was used for CO, HC, NO_x and CO₂ measurements. Total HC emissions were measured by heated flame ionization detector (FID). The CO and CO₂ emissions were determined by non-dispersive infra-red analyzers and NO_x were measured using a chemiluminescence analyzer. The equipment used are shown in Table 7.

Table 7: Regulated gaseous emissions measurement equipment.

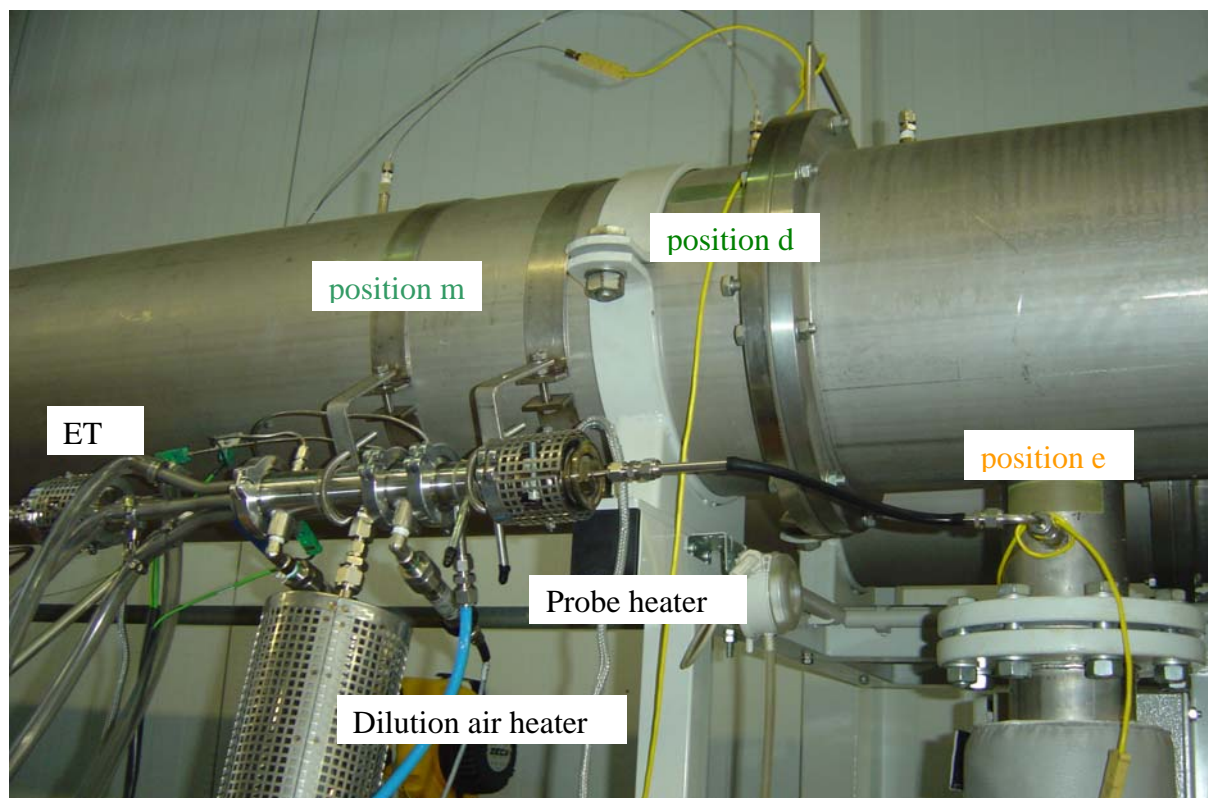
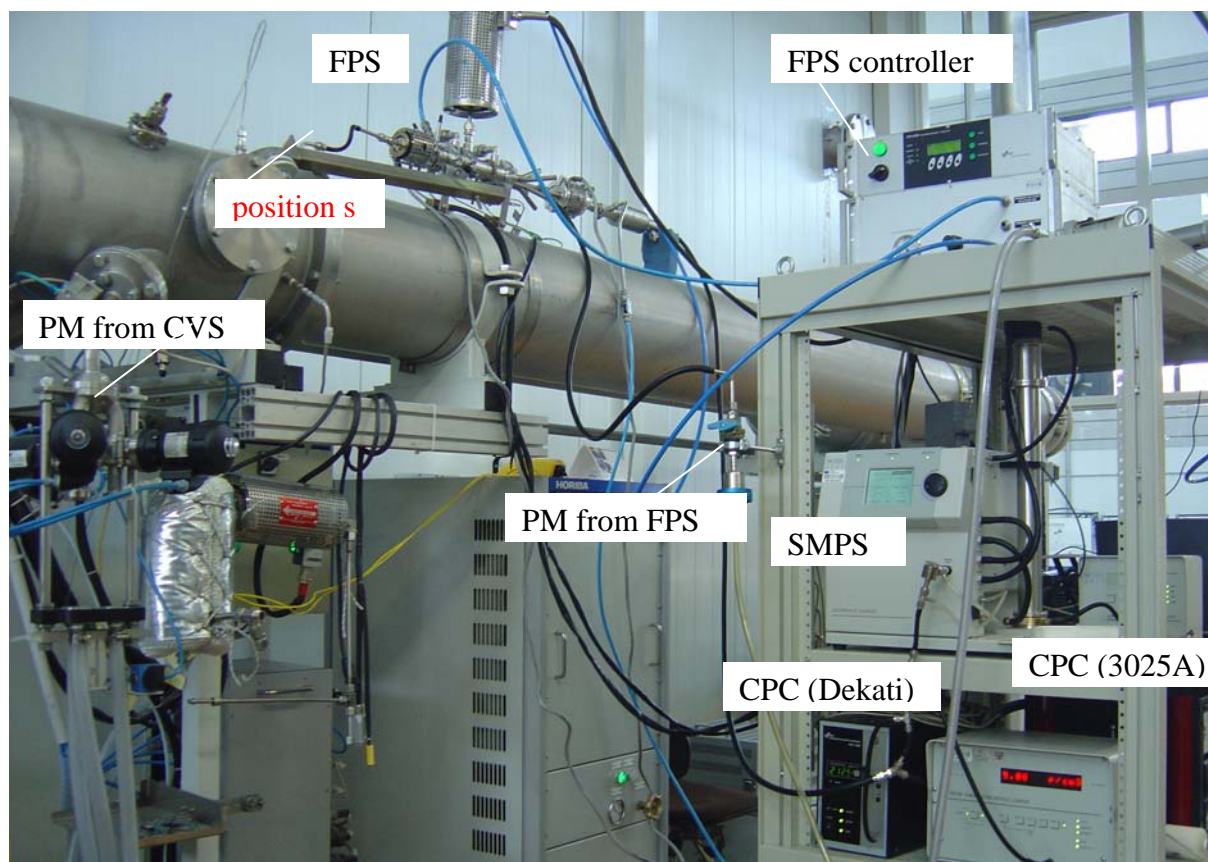
<i>Model</i>	<i>HORIBA MEXA – 7400 HTR LE</i>
THC	FID: FIA 726LE
CO	NDIR: AIA 721A
CO ₂	NDIR: AIA 772
NO _x	CLA 750 LE

STEADY-STATE TESTS

Steady-state tests of 20 min duration at 50 and 120 km/h were run. In these 20 min two CVS flow rates were tested: 6 and 12 m³/min. The detailed procedure will be given in the results section.

TEST PROTOCOL

For the whole period of the measurements (3-4 weeks) only the particular vehicle was tested in the laboratory, therefore not any artifacts due to released material from other vehicles or fuels are expected. Table 8 gives the general overview of the measurements conducted at VELA-2 for the modeling of the facilities. Figure 4 shows some characteristic photos of the set up at the various sampling positions.



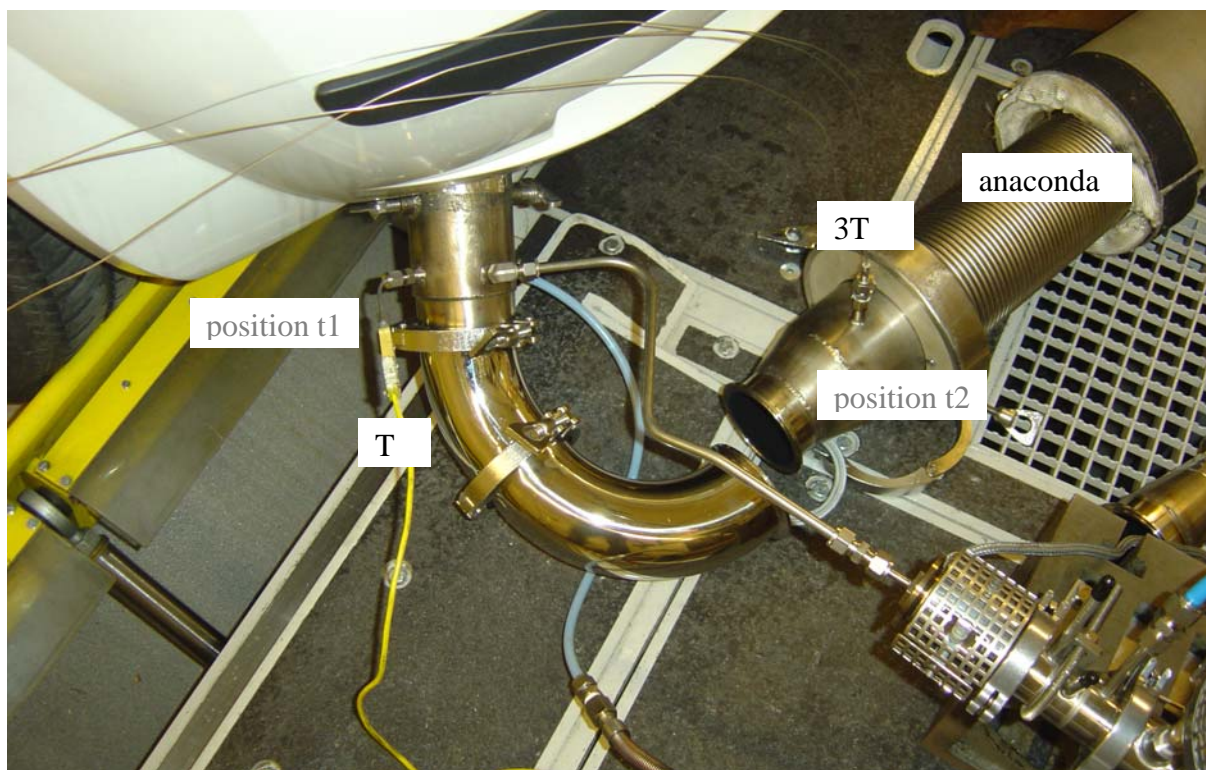


Figure 4: Examples of measurement at a) sampling position b) end of anaconda and c) tailpipe.

Table 8: Measurements for the modeling of VELA-2 facilities. 3T indicates temperature profile measurements (radial).

	DR	dilution	Speed	CVS	Probe	Depth	3T	mass	Particles file	Temperature file
15/02/2007	1-2-5	hot	50	6	s	m	s	-	070215_50_s_m	Vela2_15022007_001
	1-2-5/3	hot	50	12	s	m	s	-		
	1-2-4	hot	120	6	s	m	s	-	070215_120_s_m	Vela2_15022007_002
	1-2-4	hot	120	12	s	m	s	yes		
	1-2-3	cold	50	6	s	m	s	-	070215_50wet_s_m	Vela2_15022007_003
	1-2-3	cold	50	6	s	m	s	yes		
	1-2-6	cold	120	6	s	m	s	-	070215_120wet_s_m	Vela2_15022007_004
	1-2-6	cold	120	6	s	m	s	yes		
16/02/2007	1-2-3	hot	50	6	m	m	m	-	070216_50_m_m	Vela2_16022007_001
	1-2-3	hot	50	12	m	m	m	-		
	1-2-4	hot	120	6	m	m	m	-	070216_120_m_m	Vela2_16022007_002
	1-2-4	hot	120	12	m	m	m	-		
	1-2-3	hot	50	6	m	b	m	-	070216_50_m_b	Vela2_16022007_003
	1-2-3	hot	50	12	m	b	m	-		
	1-2-4	hot	120	6	m	b	m	-	070216_120_m_b	Vela2_16022007_004
	1-2-4	hot	120	12	m	b	m	-		
19/02/2007	1-2-3	hot	50	6	m	w	m	-	070219_50_m_w	Vela2_19022007_001
	1-2-3	hot	50	12	m	w	m	-		
	1-2-4	hot	120	6	m	w	m	-	070219_50_m_w	Vela2_19022007_002
	1-2-4	hot	120	12	m	w	m	-		
	1-2-3+	hot	50	(6/12)	e	m	d	-	070219_50_e_m	Vela2_19022007_006
	1-2-4+	hot	120	(6/12)	e	m	d	-	070219_120_e_m	Vela2_19022007_007
21/02/2007	1-2-3	hot	50	(6/12)	t	3T	d	-	070221_50_t_m	Vela2_21022007_001
	1-2-3	hot	NEDC	(12)	t	-	d	-		Vela2_21022007_002

	DR	dilution	Speed	CVS	Probe	Depth	3T	mass	Particles file	Temperature file
	1-2-4	hot	120	(6/12)	t	m+3T	d	-	070221_120_t_m	Vela2_21022007_003
	1-2-3	hot	Milan1	(12)	t	-	d	yes	070221_Milan1_t_m	
	1-2-3	hot	Milan2	(12)	t	-	d	yes	070221_Milan20_t_m	Vela2_21022007_005
	1-2-4+	cold	NM	(6/12)	t	-	d	-	070221_nm_t_m	Vela2_21022007_006
22/02/2007	1-2-3	hot	NEDC	(12)	t	-	d	yes	070222_NEDC_t_m	
	DRcheck	hot	50-120	(6/12)	t	-	d	-	070222_DR_t_m	
23/02/2007	1-2-3	hot	Artemis	(12)	s	m	s	yes	070223_Artemis_s_m	
26/02/2007	1-2-3	hot	50	6	s	m	s	-	070226_50_s_m	Vela2_26022007_001
	1-2-3	hot	50	12	s	m	s	-		
	1-2-4	hot	120	6	s	m	s	-	070226_120_s_m	Vela2_26022007_002
	1-2-4	hot	120	12	s	m	s	-		
	1-2-3	cold	50	6	s	m	s+3Te	-	070226_50wet_s_m	Vela2_26022007_003
	1-2-3	cold	50	12	s	m	s+3Te	-		
	1-2-4	cold	120	6	s	m	s+3Te	-	070226_120wet_s_m	Vela2_26022007_004
	1-2-4	cold	120	12	s	m	s+3Te	-		
27/02/2007	1-2-3	hot	50	6	s	w	s+3Te	-	070227_50_s_w	Vela2_27022007_001
	1-2-3	hot	50	12	s	w	s+3Te	-		
	1-2-4	hot	120	6	s	w	s+3Te	-	070227_120_s_w	Vela2_27022007_002
	1-2-4	hot	120	12	s	w	s+3Te	-		
28/02/2007	1-2-3	hot	50	(6/12)	e	m	m+3Te	yes	070228_50_e_m	Vela2_28022007_001
	1-2-4	hot	120	(6/12)	e	m	m+3Te	yes	070226_120_e_m	Vela2_28022007_002
01/03/2007	1-2-3	hot	-	(6/12)	da	-	-	yes	070301_back	-
	1-2-3	hot	-	-	filter	-	-	-	070301_filter	-

3. RESULTS

In the following sections the results of the measurement campaign are presented. Data are not corrected for any particle losses. In most figures the average results (from the available repetitions; see Table 3) are shown with error bars indicating \pm one standard deviation. Emissions reported are always referring to the vehicle tailpipe and are given in $[\text{cm}^{-3}]$ (i.e. corrected for CVS DR as well).

Test protocol

In order to avoid uncertainties related to different preconditioning of the vehicle the same protocols was followed for each test (Giechaskiel et al. 2007a). Figure 5 shows as an example the procedure for a 120 km/h test. Each test lasted 1180 s. For the first 780 s the CVS flow rate was 6 m^3/min and for the last 400 s 12 m^3/min . During the test, DMM and CPCs were recording continuously (Figure 6). Mass measurements were taken for around 6 min at each CVS flow rate. SMPS needs two min for each scan (90 s for the up scan and 30 s for the down scan) so approximately 5 scans were taken the first 780 s and 3 the next 400 s. The first 380 s of the test were considered as warm up phase so any measurements during this period were not taken into account.

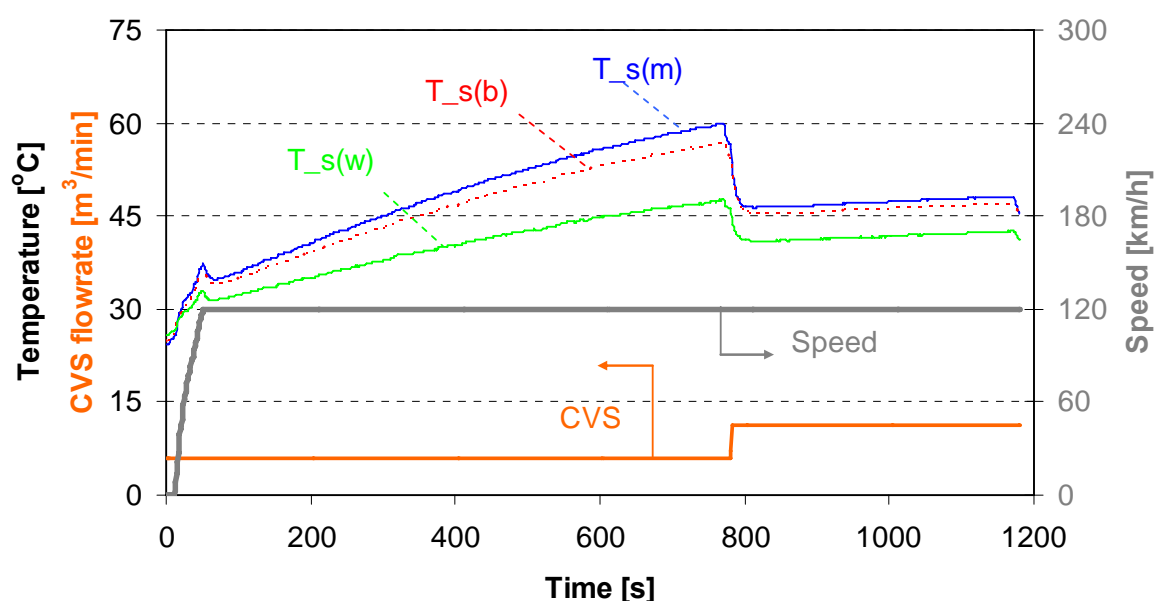


Figure 5: Typical measurement: temperature data.

File “CVS_protocol2” (and Figure 7 as an example) gives the averages of all instruments and temperatures during the 90 s that the SMPS was measuring. Then for the final results of this report only the 3 SMPS scans measured during the “stabilized” 400 s are taken into account. The error bars indicate always the variation of the 3 SMPS scans or the 3 averages of the instruments during the 3 SMPS scans.

The raw and corrected for dilution averaged results are given in the xls file “CVS_protocol2”, which is available upon request.

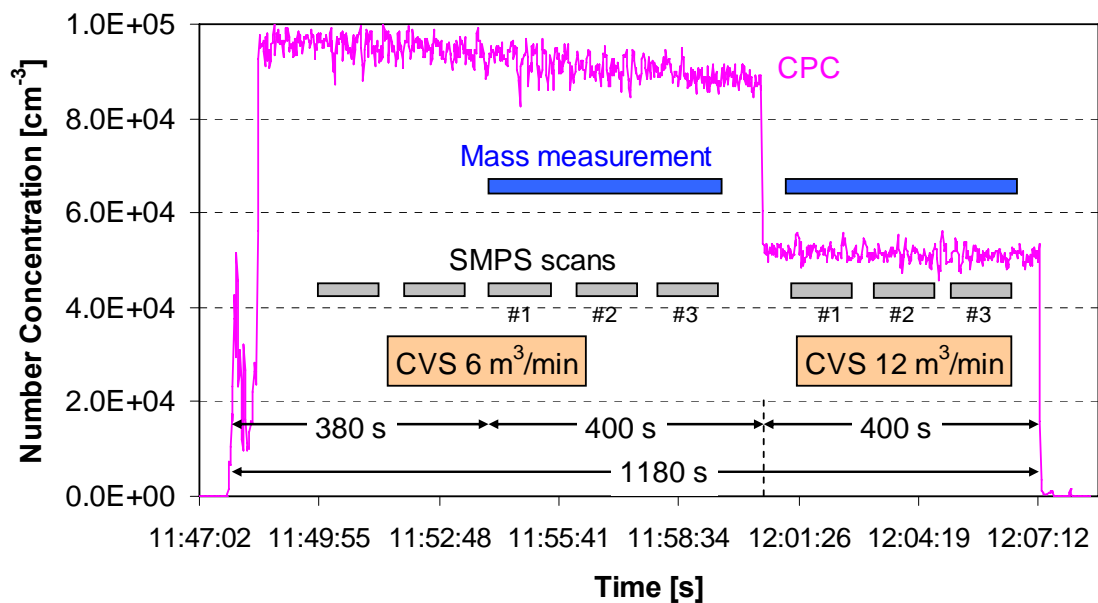


Figure 6: Typical measurement: particle instruments data.

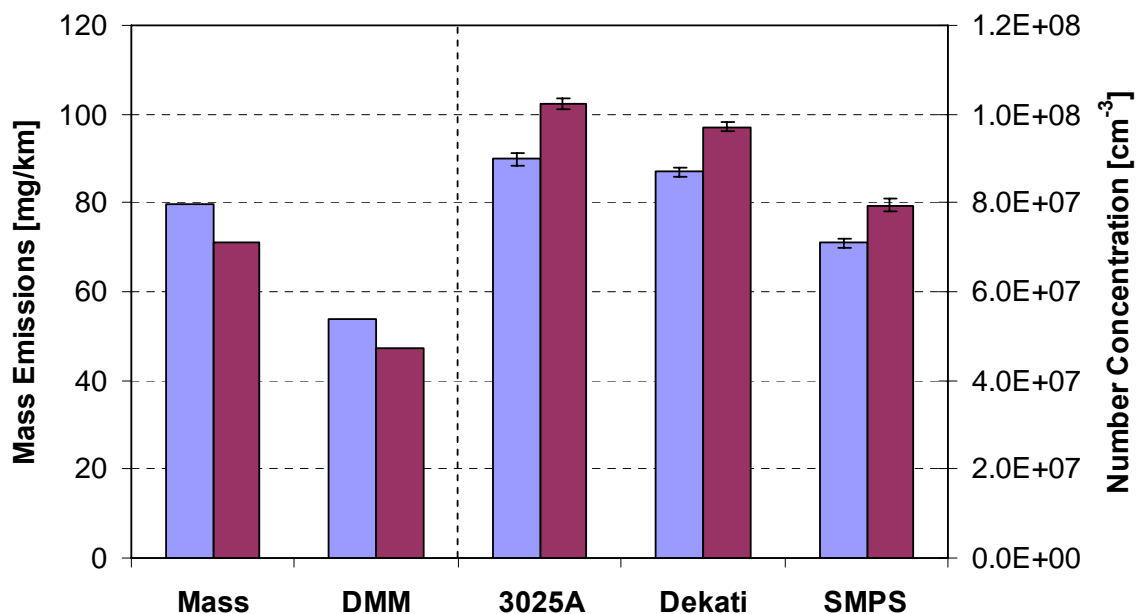


Figure 7: Results of the measurements of the previous Figure for the Mass, CPC (3025A) and SMPS. The Mass is calculated from the weight on the filter corrected for the dilution ratio (DR), CVS flow-rate, and vehicle speed. SMPS is the average of the 3 scans corrected for FPS DR and the CVS DR. CPC is the average from the times that the 3 SMPS scans were taken (corrected for the FPS DR and the CVS DR).

Stability

The stability of the measurements (for DMM, CPC 3025A, CPC Dekati and total concentration of SMPS) can be checked with the Coefficient of Variance ($CoV = \text{stdev}/\text{mean}$). Usually it was better than 5% with the exception of some measurements at the mixing point (between) where it was around 10%. These values are within common experimental uncertainties.

For SMPS the size dependent stability was also checked. Figure 8 shows a size distribution and the mean variation at 50 and 120 km/h. Between 40 and 200 nm the CoV is <10%. Outside this range the concentration of particles is very low leading to high CoVs.

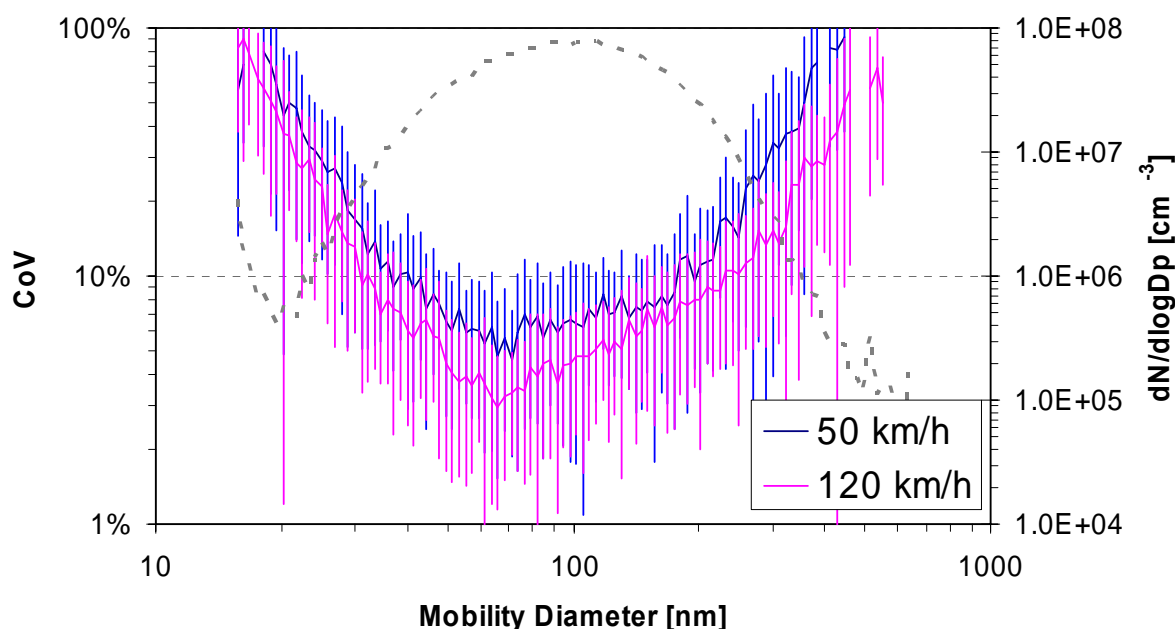


Figure 8: Stability of SMPS size distribution results.

Repeatability

The repeatability of the measurements was checked by comparing the results at the same sampling position of two different days (beginning and end of measurement campaign). Figure 9 shows the results at the sampling position sampling point (middle) for 120 km/h where the FPS was used with exactly the same settings and temperatures. Two cases corresponding at CVS flow rate of 6 and 12 m³/min are shown. Red lines are the results of the first period and green lines for the second after a -10% correction. The size distributions are exactly the same (mean, stdev) indicating no change of the size distribution. The -10% difference of the concentration can be attributed to the dirtiness of the sampling device (FPS and ejector) or uncertainties in the ejector dilution air pressure setting. The second repeat was conducted after the sampling system had measured at the tailpipe. When the sampling system get's dirty its dilution ratio increases and this cannot be taken into account from the instruments dilution ratio indication. The results presented in this report have been corrected for this -10% for the second period of measurements (after the measurements at the tailpipe) when used.

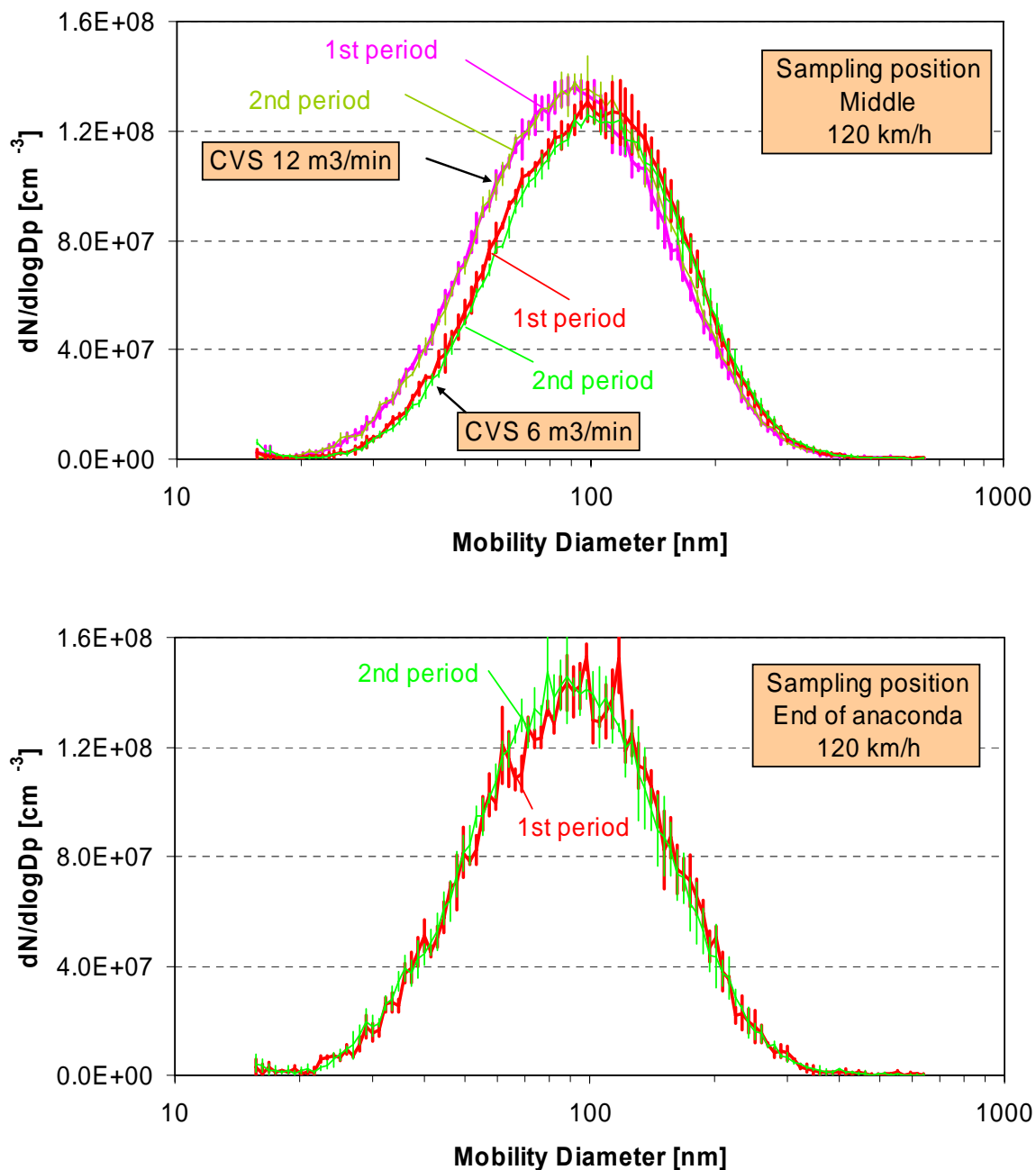


Figure 9: Repeatability of measurements at 120 km/h a) at CVS b) at the end of anaconda.

Wet – dry measurements (Cold – Hot dilution)

Most measurements were conducted with the PMP protocol. According to this protocol only non volatile particles are measured as the FPS measures with hot dilution and an evaporation tube. However some measurements were conducted with cold dilution and ambient temperature at the evaporation tube. These conditions are supposed to favor the creation of a nucleation mode.

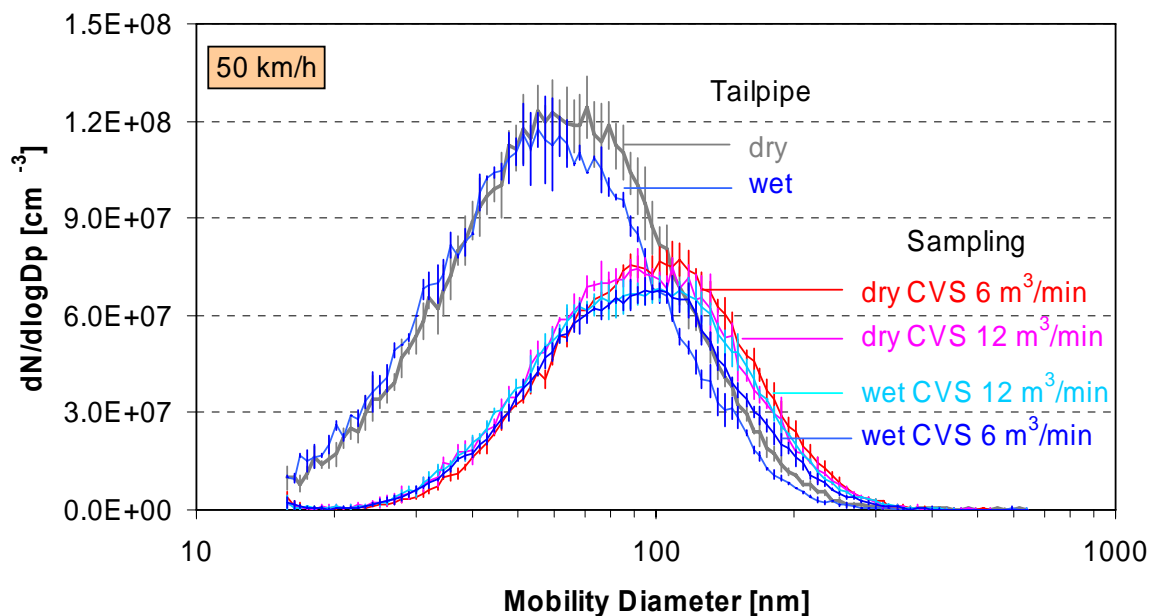


Figure 10: Comparison of wet and dry measurement for 50 km/h at different sampling positions (always in the middle of the tube).

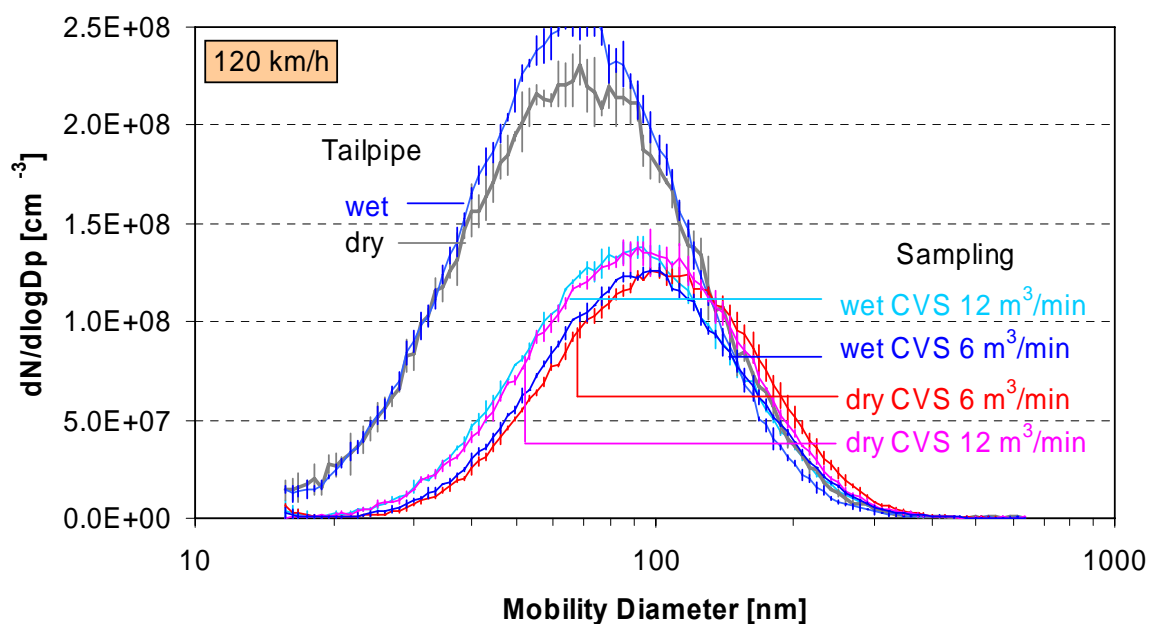


Figure 11: Comparison of wet and dry measurement for 120 km/h at different sampling positions (always in the middle of the tube).

The comparison of cold and hot dilution (or wet and dry particles) for 50 km/h is shown in Figure 10. The wet results shown are *corrected for -40%*. This correction can be explained by the higher ejector dilutor sample coming in at low temperatures due to the higher density of the sample gas (Giechaskiel et al. 2004). There is no difference between wet and dry size distributions at CVS (within the experimental uncertainties). Figure 11 shows the results for the 120 km/h (again with a -40% correction at the wet measurements). In this case there are small differences between wet and dry measurements indicating that there might be particle losses when using the hot dilution or that the correction used is lower than it should.

As both wet and dry size distributions were unimodal and there was not a significant change in the size distribution the above mentioned issues were not further investigated. The presence of a single mode can be explained by the low sulfur fuel level and the high efficiency of the oxidation catalyst (Giechaskiel et al. 2005). Heating the mass filters showed that the volatile fraction of the filters was 8% and 12% for 50 and 120 km/h respectively. This indicates that there is only a small amount of condensable material in the exhaust gases.

Effect of sampling position

Figure 12 and Figure 13 show the size distributions measured at 50 and at 120 km/h at the tailpipe, end of anaconda and sampling point. It is evident that the main change takes place in the transfer tube (anaconda) where a big change of the peak is observed.

Figure 14 (for 50 km/h) and Figure 15 (for 120 km/h) show the total particle concentrations for the SMPS and the two CPCs. There is a decrease of the particle concentration from the tailpipe to the final sampling point.

Table 9 summarizes the results from all measurements from SMPS.

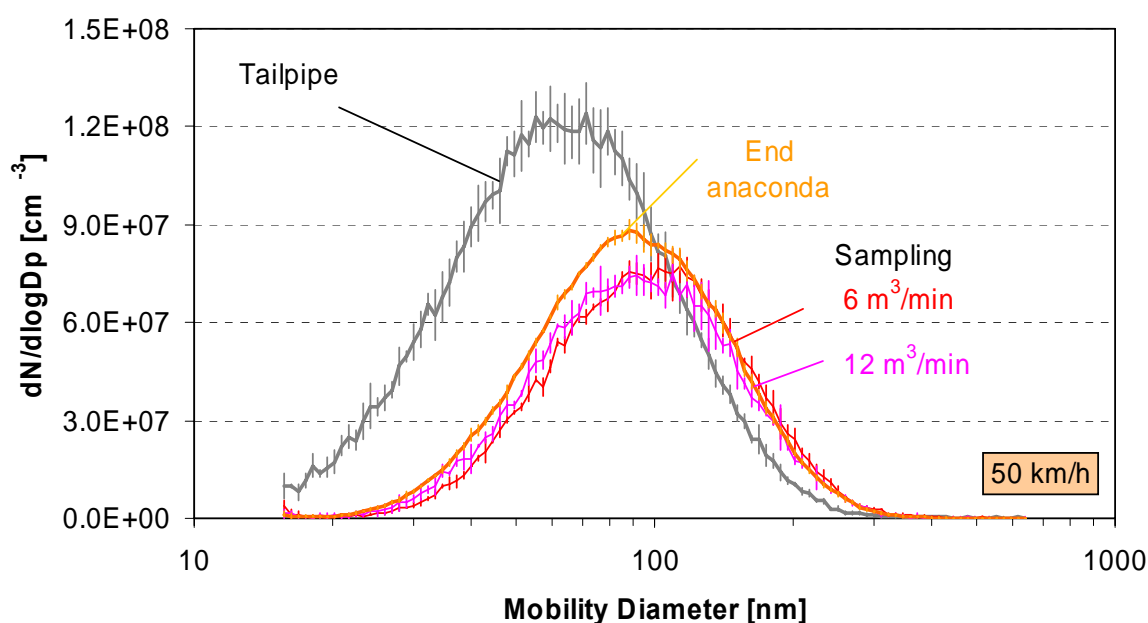


Figure 12: Size distributions at different sampling positions (middle of tube) for 50 km/h.

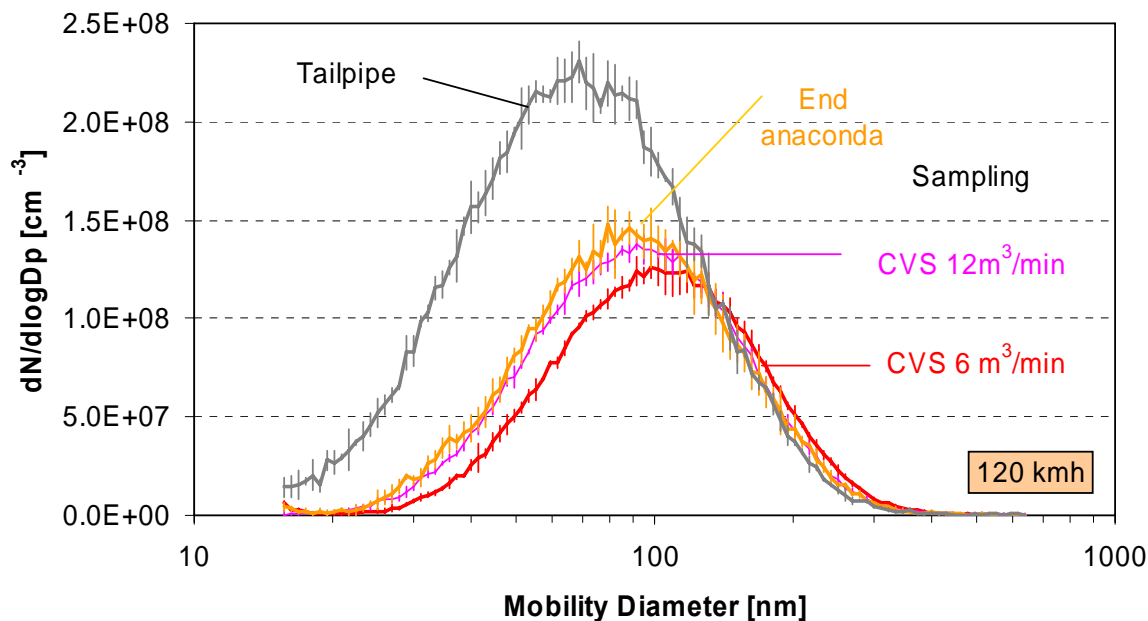


Figure 13: Size distributions at different sampling positions (middle of tube) for 120 km/h

At 50 km/h the geometric mean of the size distribution changes from approximately 61 nm (tailpipe) to 85-88 nm (end anaconda) (Figure 14). When the exhaust gas enters the CVS no size distribution change is observed at 50 km/h for the high CVS flow rate (apart from the decrease of the concentration due to dilution). In the case of low CVS flow rate a small change is observed (increase of peak and decrease of concentration).

At 120 km/h the peak of the size distribution changes from approximately 66 nm (tailpipe) to 87 nm (end anaconda) (Figure 15). At CVS the peak slightly increases in the case of high CVS flow rate (89 nm) but a lot in the case of low CVS flow rate (98nm).

Figure 16 (for 50 km/h) and Figure 17 (for 120 km/h) show the mass results from the filter measurements, the DMM and the SMPS where the density was given from the equation (fitting the data from Maricq and Xu 2004):

$$\text{Particle Density in g/cm}^3 = -0.3825 \times \log(\text{Diameter in nm}) + 2.52$$

This equation gives a density of 1 g/cm³ at 50 nm and 0.23 g/cm³ at 400 nm. Generally there is a good agreement (within experimental uncertainties) of the masses calculated at different sampling positions indicating that the losses in the anaconda and CVS shouldn't be high. This 10% underestimation of the mass at the tailpipe at both 50 and 120 km/h is probably dilution ratio uncertainty.

Table 9: Summary of SMPS results for 50 km/h and 120 km/h

Probe position		Speed	CVS flow	FPS	D (nm)	+/-	CoV	N (#/cc)	+/-	CoV
Sampling point	Middle	50	5.85	hot	89.4	1.4	2%	3.66E+07	1.40E+06	4%
Sampling point	Middle	50	11.4	hot	84.2	0.9	1%	3.73E+07	1.59E+06	4%
Sampling point	Middle	50	5.85	cold	84.9	0.3	0%	3.63E+07	3.09E+05	1%
Sampling point	Middle	50	11.4	cold	81.3	1.3	2%	3.72E+07	2.99E+06	8%
Mixing Point	Middle	50	5.85	hot	85.6	1.4	2%	5.21E+07	8.05E+05	2%
Mixing Point	Middle	50	11.4	hot	82.9	0.9	1%	5.03E+07	1.82E+06	4%
Mixing Point	Between	50	5.85	hot	87.8	2.8	3%	2.23E+07	1.04E+06	5%
Mixing Point	Between	50	11.4	hot	82.4	1.4	2%	2.25E+07	3.88E+05	2%
Mixing Point	Walls	50	5.85	hot	88.3	0.6	1%	2.36E+07	4.17E+05	2%
Mixing Point	Walls	50	11.4	hot	85.3	0.7	1%	2.54E+07	5.57E+04	0%
End anaconda	Middle	50	5.85	hot	85.4	0.7	1%	4.53E+07	1.64E+06	4%
Tailpipe	Middle	50	11.4	hot	61.4	1.0	2%	7.42E+07	3.90E+06	5%
Tailpipe	Middle	50	5.85	cold	57.2	0.4	1%	6.94E+07	1.40E+06	2%
Sampling point	Middle	50	5.85	hot	94.2	1.2	1%	4.09E+07	1.04E+06	3%
Sampling point	Middle	50	11.4	hot	89.3	1.7	2%	4.09E+07	5.47E+05	1%
Sampling point	Middle	50	5.85	cold	87.5	1.4	2%	3.62E+07	5.50E+05	2%
Sampling point	Middle	50	11.4	cold	89.1	1.0	1%	3.95E+07	4.79E+05	1%
Sampling point	Walls	50	5.85	hot	92.7	1.2	1%	3.92E+07	7.71E+05	2%
Sampling point	Walls	50	11.4	hot	88.3	0.9	1%	3.93E+07	1.36E+06	3%
End Anaconda	Middle	50	5.85	hot	88.6	1.6	2%	5.17E+07	5.52E+05	1%
End Anaconda	Middle	50	11.4	hot	87.6	0.8	1%	4.67E+07	1.25E+05	0%

Probe position		Speed	CVS flow	FPS	D (nm)	+/-	CoV	N (#/cc)	+/-	CoV
Sampling point	Middle	120	5.85	hot	98.2	2.1	2%	7.25E+07	1.81E+06	2%
Sampling point	Middle	120	11.4	hot	88.9	1.5	2%	7.70E+07	1.35E+06	2%
Sampling point	Middle	120	5.85	cold	96.5	2.5	3%	7.78E+07	3.10E+06	4%
Sampling point	Middle	120	11.4	cold	88.4	0.6	1%	8.70E+07	3.97E+05	0%
Mixing Point	Middle	120	5.85	hot	92.7	2.9	3%	6.75E+07	3.41E+06	5%
Mixing Point	Middle	120	11.4	hot	86.3	1.0	1%	9.64E+07	3.33E+06	3%
Mixing Point	Between	120	5.85	hot	92.6	2.6	3%	4.23E+07	1.17E+06	3%
Mixing Point	Between	120	11.4	hot	85.7	1.0	1%	4.23E+07	1.32E+06	3%
Mixing Point	Walls	120	5.85	hot	93.4	1.6	2%	5.12E+07	1.32E+06	3%
Mixing Point	Walls	120	11.4	hot	85.8	1.5	2%	4.79E+07	1.51E+06	3%
End anaconda	Middle	120	5.85	hot	95.1	0.9	1%	9.49E+07	1.41E+06	1%
Tailpipe	Middle	120	11.4	hot	67.4	0.9	1%	1.42E+08	2.30E+06	2%
Tailpipe	Middle	120	11.4	cold	65.8	0.7	1%	1.49E+08	2.01E+06	1%
Sampling point	Middle	120	5.85	hot	99.2	1.9	2%	7.02E+07	9.67E+05	1%
Sampling point	Middle	120	11.4	hot	90.0	0.9	1%	7.85E+07	1.47E+06	2%
Sampling point	Middle	120	5.85	cold	92.7	1.2	1%	6.71E+07	6.44E+04	0%
Sampling point	Middle	120	11.4	cold	86.2	0.6	1%	7.62E+07	2.26E+04	0%
Sampling point	Walls	120	5.85	hot	100.3	2.0	2%	6.56E+07	7.41E+05	1%
Sampling point	Walls	120	11.4	hot	88.9	1.4	2%	7.26E+07	1.85E+06	3%
End Anaconda	Middle	120	5.85	hot	87.2	2.6	3%	8.23E+07	3.79E+06	5%
End Anaconda	Middle	120	11.4	hot	80.4	1.2	2%	6.89E+07	1.30E+06	2%

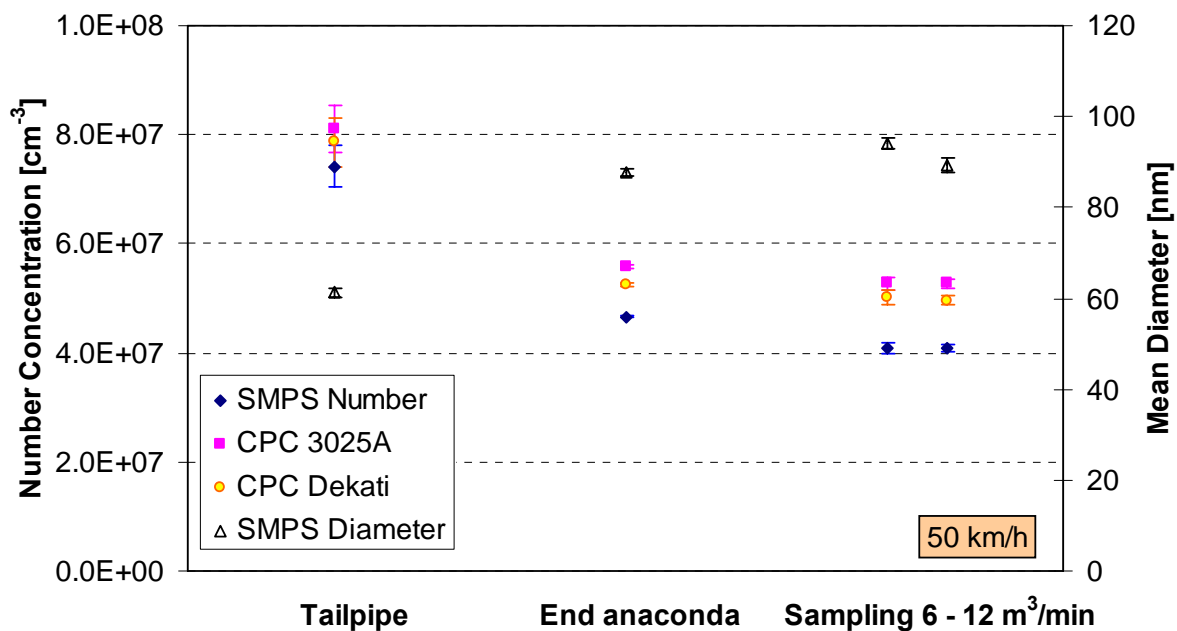


Figure 14: Concentration and mean diameter at different sampling positions at 50 km/h.

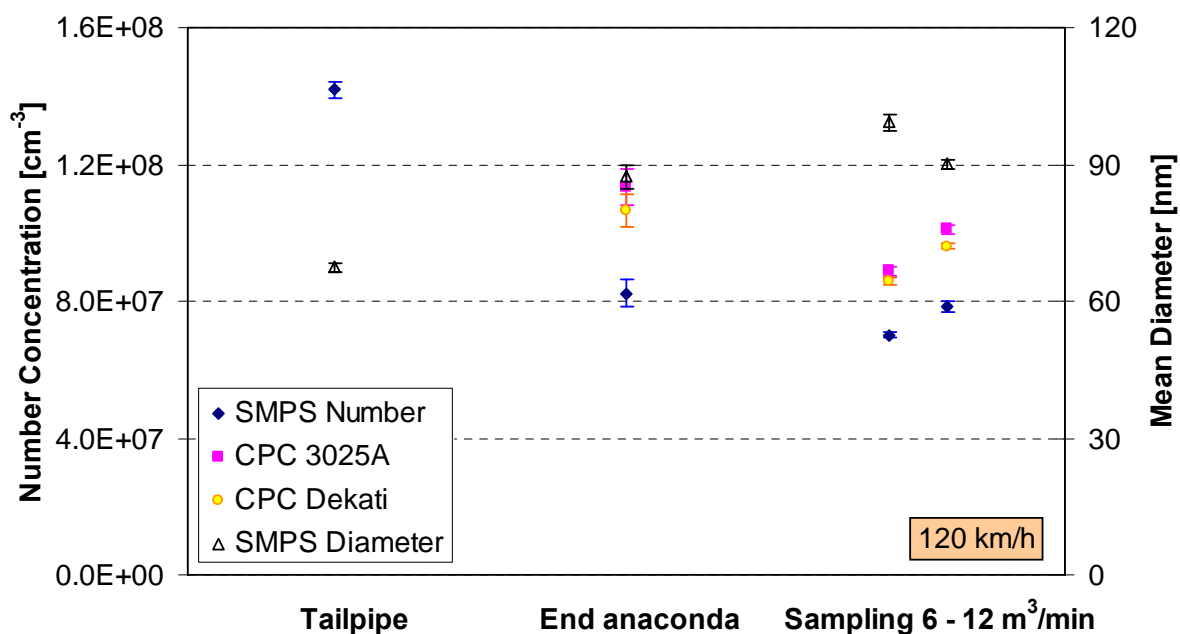


Figure 15: Concentration and mean diameter at different sampling positions at 120 km/h.

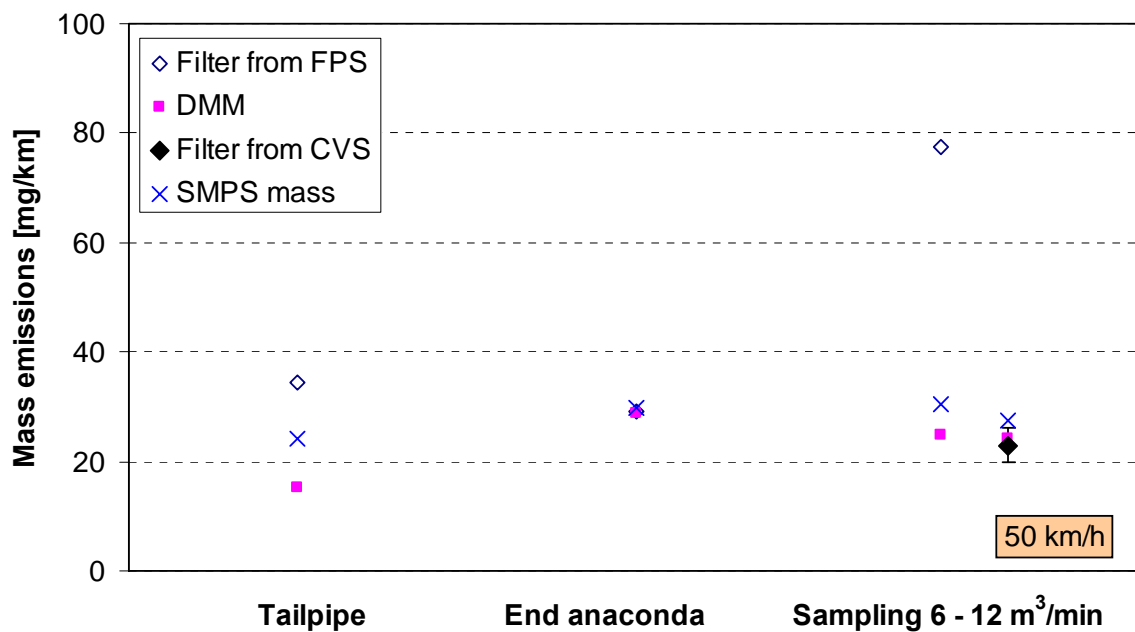


Figure 16: Mass results at different sampling positions for the case of 50 km/h.

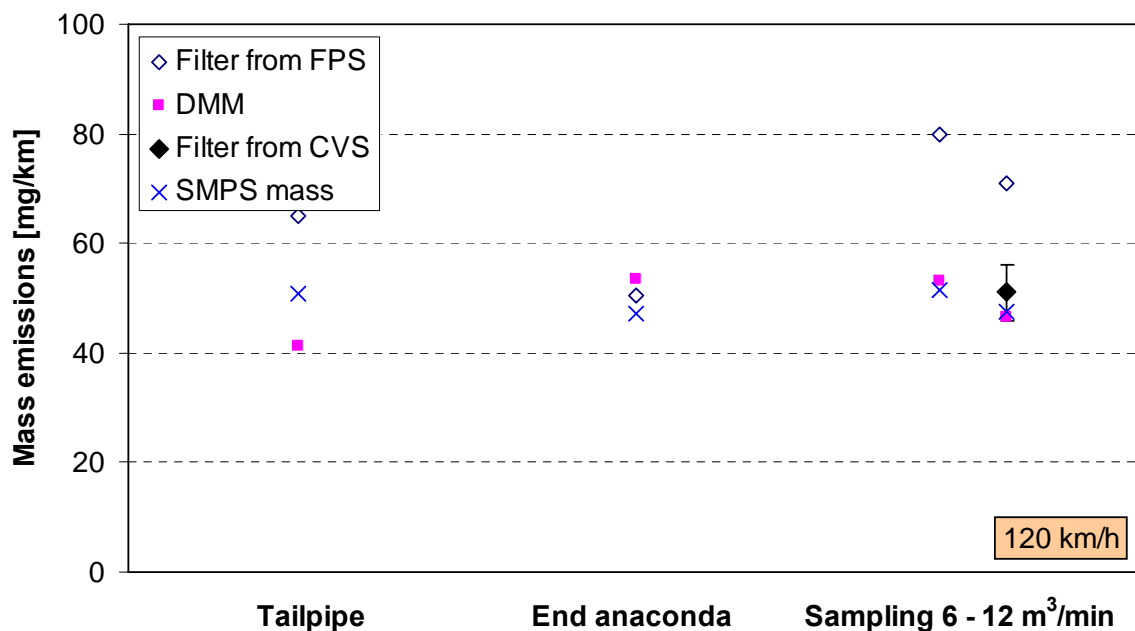


Figure 17: Mass results at different sampling positions for the case of 120 km/h.

Mixing point

At the mixing point (1.5 tunnel diameters downstream the entrance of the exhaust gas in the CVS) the mixing of the two flows is not complete. Figure 18 and Figure 19 also show the % correction necessary to match the size distributions in CVS with the size distribution at the end of anaconda. It is interesting to note the lower than anticipated mixing in the between position. This has probably to do with the turbulence created in the area. Similar strange behavior is observed for the temperatures as well (see Appendix D and E).

It is also interesting to note that in the case of high particle number concentration (120 km/h) and low CVS dilution ratio (6 m³/min) the size distribution has already changed at the mixing point (peak of the accumulation mode increased to bigger diameters).

Temperature profiles

Temperatures were measured at different sampling positions and at different radial positions. The real time change of the profiles and the radial profiles are given in Appendices D and E. It must be emphasized that the temperatures seem that they never reached a steady-state as they were always increasing. This had to do probably due to the long lasting heating of the metal parts of the facilities (anaconda, dilution tunnel). However they were very repeatable at different days as the negligible error bars of the figures show.

One point that needs special attention is the lower than 60°C temperature at the end of anaconda (Figure D1). This has to do with the fact that the heating of the anaconda was turned on with the beginning of the measurement at 50km/h and for this reason the tube was at ambient temperature.

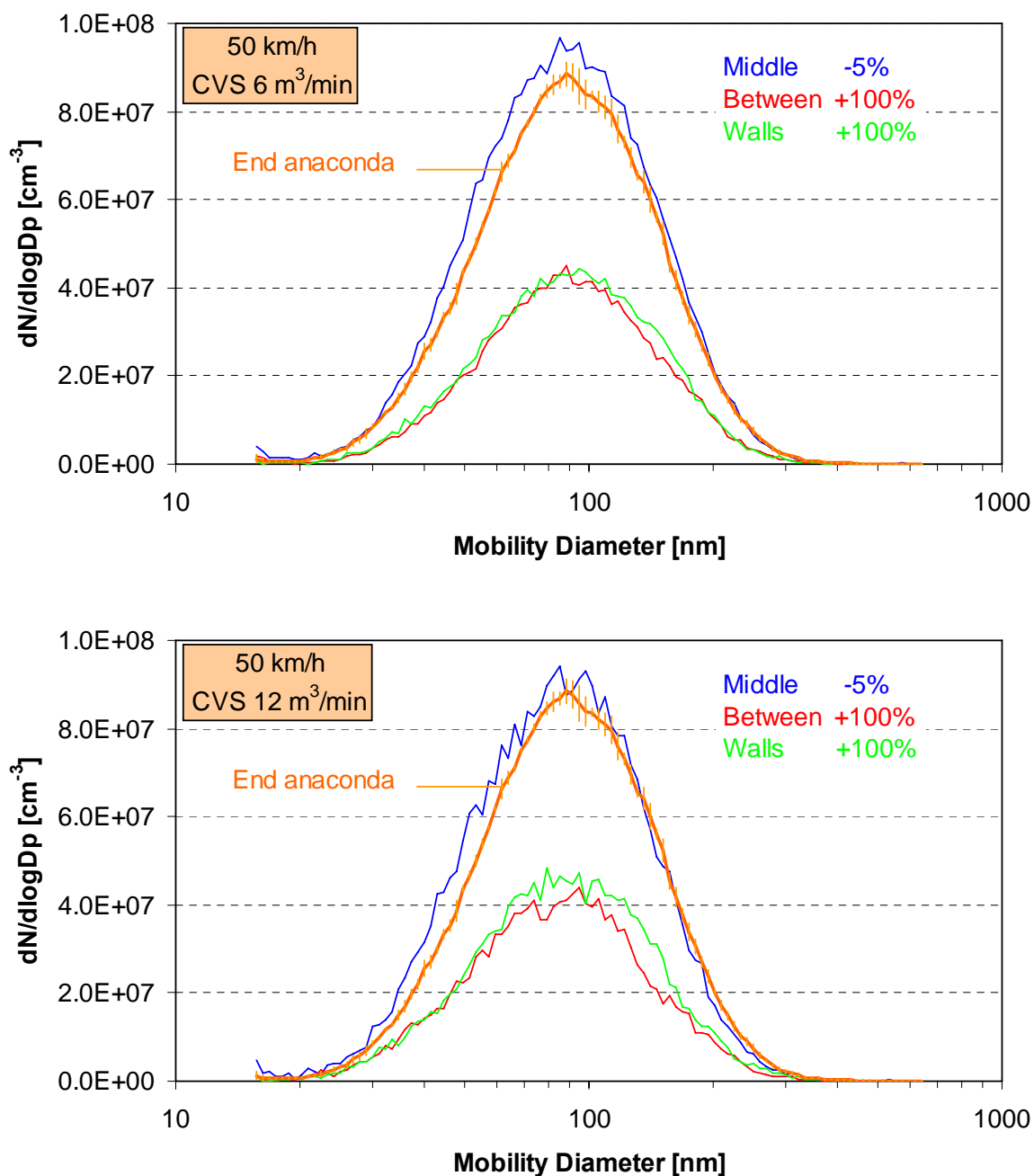


Figure 18: Size distributions at the end of anaconda and at different radial positions at the mixing position at CVS. Percentages show the necessary CVS correction at the mixing point to match the “inlet” (end anaconda) size distribution.

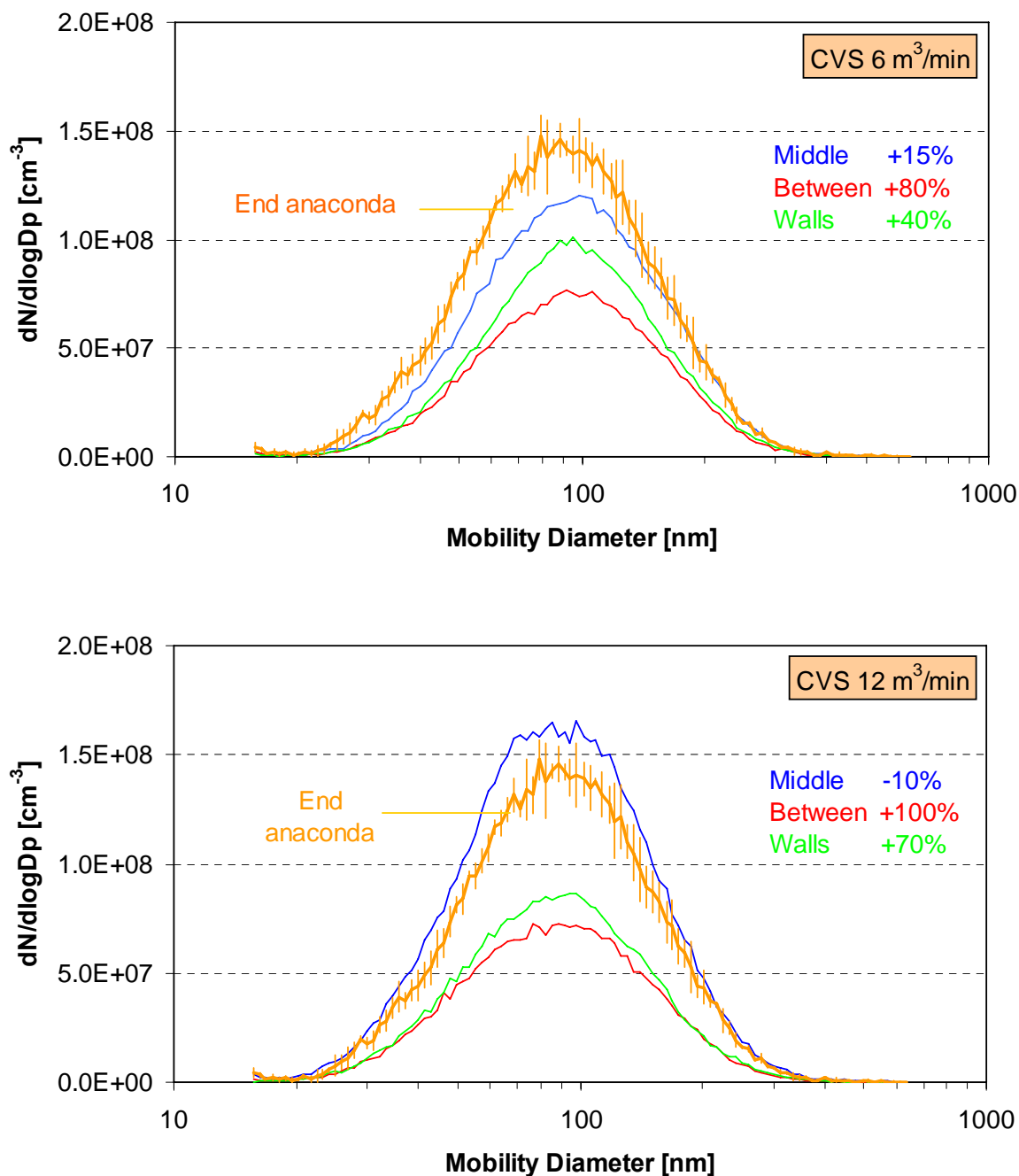


Figure 19: Size distributions at the end of anaconda and at different radial positions at the mixing position at CVS. Percentages show the necessary CVS correction at the mixing point to match the “inlet” (end anaconda) size distribution. CVS flow rate a) 6 and b) 12 m³/min.

Comparison of instruments

The two CPCs used for the measurements (TSI 3025A and Dekati prototype) correlated very well (Figure 20). The SMPS underestimated the emissions approximately 20% (Figure 21). This difference is acceptable as the SMPS measures particles in the size range of 10-300 nm, while CPCs from 3 up to some micros. The comparison of the DEKATI prototype with the TSI SMPS gives the same results. Figure 22 is in a linear scale and the 20% difference is more evident. It's also important to note that for particle number concentrations up to 2×10^5 (double than its upper limit) the DEKATI CPC measures precisely and the linear correlation is valid (with the 20% difference). It is worth mentioning that SMPS had a small leakage and couldn't zero. For this reason it had a background of 30 particles/cm³. This [background](#) was taken into account in the results, however it affected only slightly the results.

The correlation between DMM and SMPS was also satisfactory with an $R^2=0.9$ (Figure 23). DMM measures mass combining mobility and aerodynamic size distributions to calculate a density of particles. SMPS measures number concentration.

DMM (and CPCs) however do not correlate well with the mass measurements from the FPS (Figure 24). This has to do with the low mass amount collected on the filters due to the high dilution and the small sampling time (5 min). Typical mass collected on the filter was 50 µg. For this reason the mass results from FPS are not considered in this report. However, when DMM was compared with the PM from the CVS the correlation improved ($R^2=0.67$). Moreover the slope is close to 1 (1.085). If only the non-volatile fraction of the PM is considered (~90%) then the relation is almost excellent.

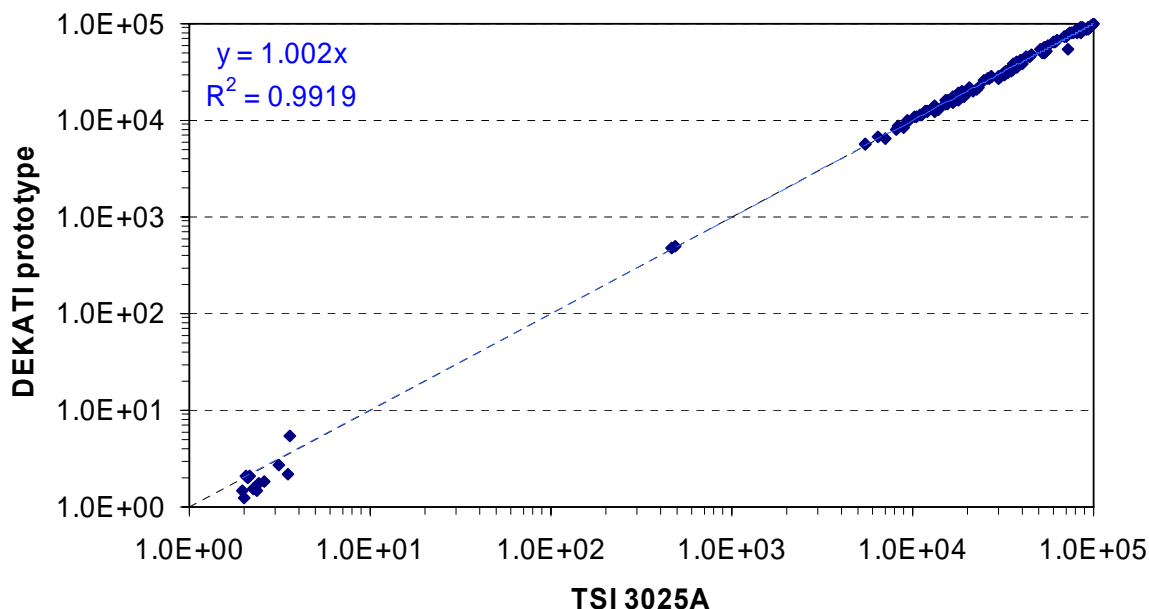


Figure 20: Correlation between the two CPCs used in the study.

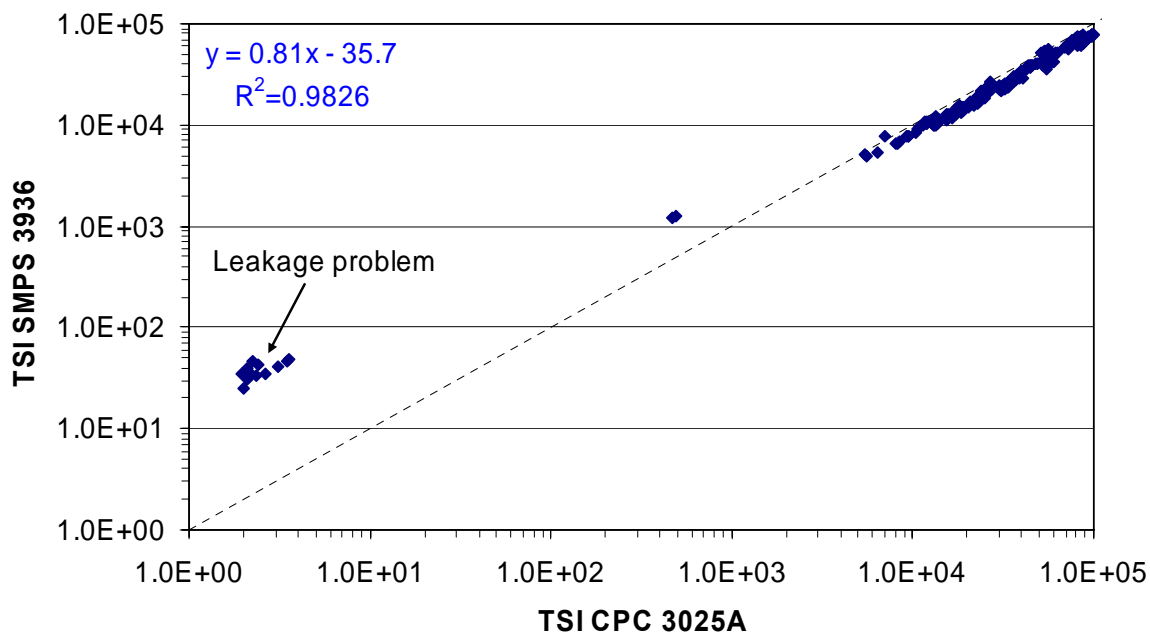


Figure 21: Correlation between TSI's CPC and SMPS.

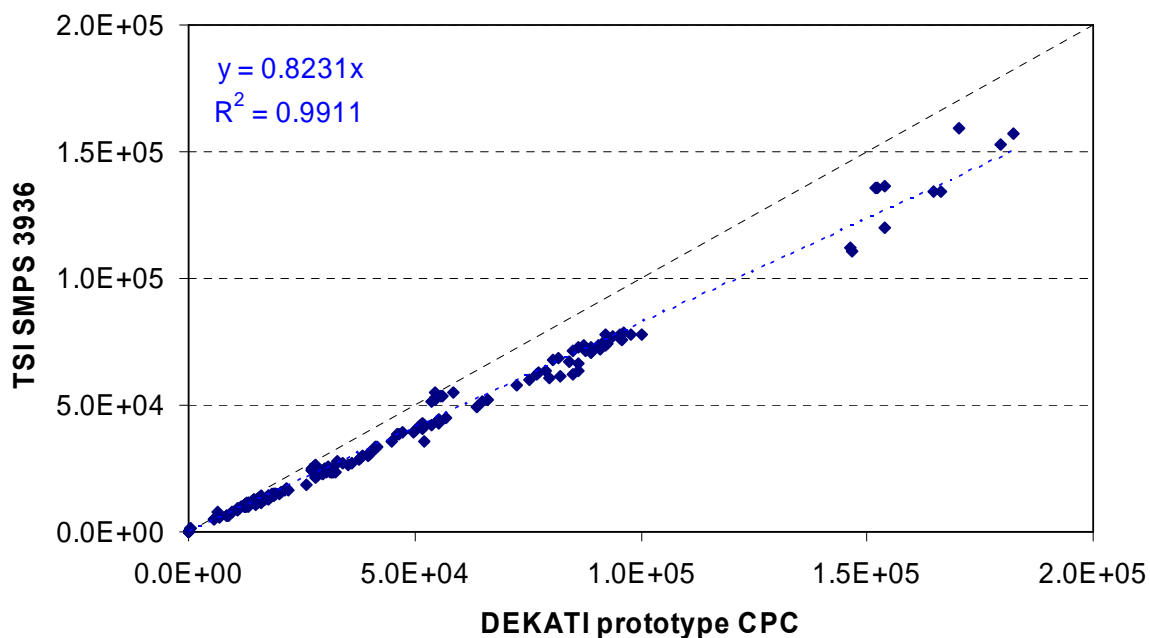


Figure 22: Correlation between DEKATI's CPC and TSI's SMPS.

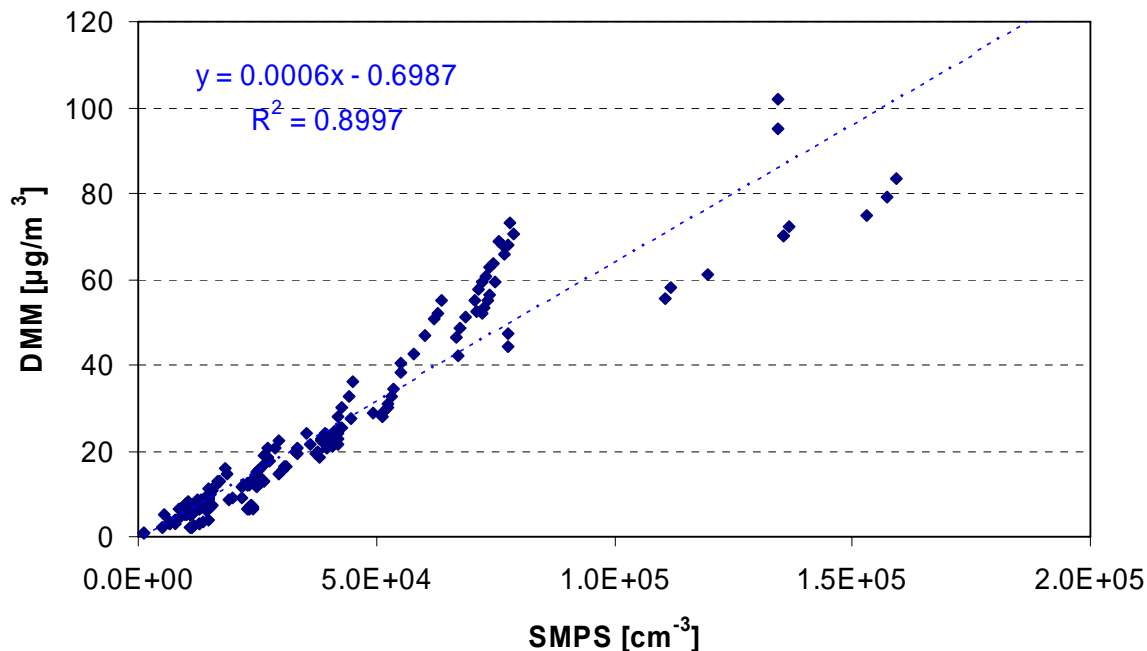


Figure 23: Correlation between DMM and SMPS.

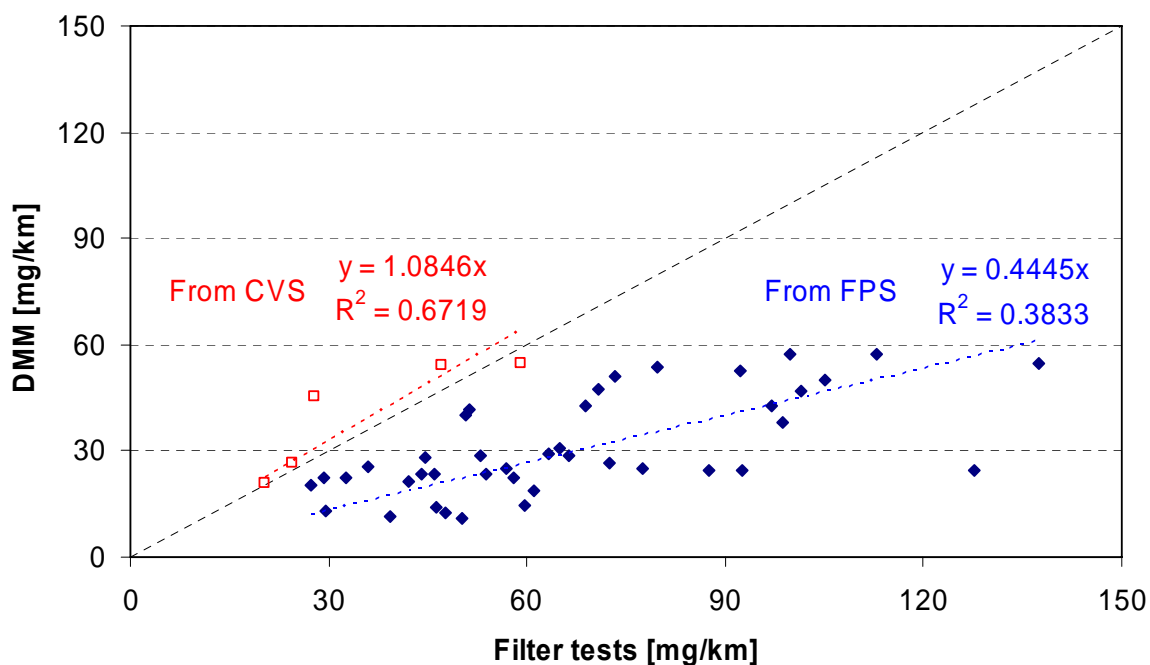


Figure 24: Correlation between DMM and filter measurements. There is a poor correlation with the FPS mass results due to the low mass collected on the filters. There is a very good correlation with the CVS results.

REFERENCES

- Andersson, J., Giechaskiel B., Munoz-Bueno, R., Dilara, P. (2007). Particle Measurement Programme (PMP): Light-duty Inter-laboratory Correlation Exercise (ILCE_LD)-Final report (EUR 22775 EN) GRPE-54-08-Rev.1, <http://www.unece.org/trans/main/wp29/wp29wgs/wp29grpe/grpeinf54.html>
- Baron, P. A., Willeke, K. (2001). Aerosol Measurement: Principles, Techniques, and Applications, 2nd edition, Wiley-Interscience, ISBN 0-471-35636-0
- Casati, R., Scheer, V., Vogt R, Benter, T. (2007). Measurement of nucleation and soot mode particle emission from a diesel passenger car in real world and laboratory in situ dilution. Atmospheric Environment, 41, 2125-2135
- Dekati Ltd, <http://www.dekati.fi/>
- Giechaskiel, B., Munoz-Bueno, R., Rubino, L., Dilara, P., Urbano, M., Andersson, J. (2007b). Emissions of a Euro 4 light-duty diesel vehicle equipped with DPF. Close examination of particle size distributions during regeneration. SAE 2007-01-1944.
- Giechaskiel, B., Ntziachristos, L., Samaras, Z., Casati, R., Scheer, V., Vogt, R. (2005). Formation Potential of Vehicle Exhaust Nucleation Mode Particles On-Road and in the Laboratory, Atmospheric Environment, 39, 3191-3198
- Giechaskiel, B., Ntziachristos, L., Samaras, Z., Casati, R., Volker, S., Rainer, V. (2007a). Effect of speed and speed transition on the formation of nucleation mode particles from a light duty diesel vehicle. SAE 2007-01-1110.
- Giechaskiel, B., Ntziachristos, L., Samaras Z. (2004). Calibration and Modeling of Ejector Dilutors for Automotive Exhaust Sampling, Measurement Science & Technology, 15, 2199-2206
- Good P. (2007). An Overview of European Emissions Legislation for LD vehicles. Presentation at the International Conference on transport and Environment, Milan 19-21 March 2007, Italy, available at http://transportenv07.jrc.it/proceedings_D.html
- Hinds, W. C. (1999). Aerosol Technology, New York: McGrawHill
- Maricq, M., Chase, R., Podsiadlik, D., Vogt, R. (1999). Vehicle Exhaust particle Size Distributions: A Comparison of Tailpipe and Dilution Tunnel Measurements. SAE 1999-01-1461
- Maricq, M., Xu, N. (2004). The effective density and fractal dimension of soot particles from premixed flames and motor vehicle exhaust. J. Aerosol Science 35, 1251-1274
- Ntziachristos, L., Giechaskiel, B., Pistikopoulos, P., Samaras, Z. (2005). Comparative Assessment of Two Different Sampling Systems for Particle Emission Type-Approval Measurements, SAE Transactions 2005-01-0198
- Ntziachristos, L., Giechaskiel, B., Pistikopoulos, P., Samaras, Z., Mathis, U., Mohr, M., Ristimäki, J., Keskinen, J., Mikkanen, P., Casati, R., Scheer, V., Vogt, R. (2004). Performance Evaluation of a Novel Sampling and Measurement System for Exhaust Particle Characterization. SAE 2004-01-1439.
- Reg. 83 - Rev.3 - Emission of Pollutants According to Engine Fuel Requirements, <http://www.unece.org/trans/main/wp29/wp29regs81-100.html>

TSI Incorporated, <http://www.tsi.com/>

Vogt, R., Scheer, V. (2002). Particles in diesel vehicle exhaust: A comparison of laboratory and chasing experiments Proceedings of the 11th International Symposium Transport and Air Pollution, Graz 19-21.6.2002, pp 79-84, Univ.-Prof. Dr. R. Pischinger, Graz, ISBN 3-901351-59-0

DEFINITIONS, ACRONYMS, ABBREVIATIONS

CPC:	Condensation Particle Counter
CVS:	Constant Volume Sampler
DMA:	Differential Mobility Analyser
DMM:	Dekati Mass Monitor
DR:	Dilution Ratio
ET:	Evaporation Tube
FPS:	Fine Particle Sampler
JRC:	Joint Research Centre
PMP:	Particle Measurement Programme
SMPS:	Scanning Mobility Particle Sizer
VELA:	Vehicles Emissions Laboratory

ANNEXES

A. FPS and Ejector dilutors

The particle sample into the FPS is extracted from an undiluted aerosol, e.g., tailpipe (Figure A1). The first (primary) dilution is conducted inside a perforated tube. The operation principle is shown in Figure A2 (Dekati FPS manual).

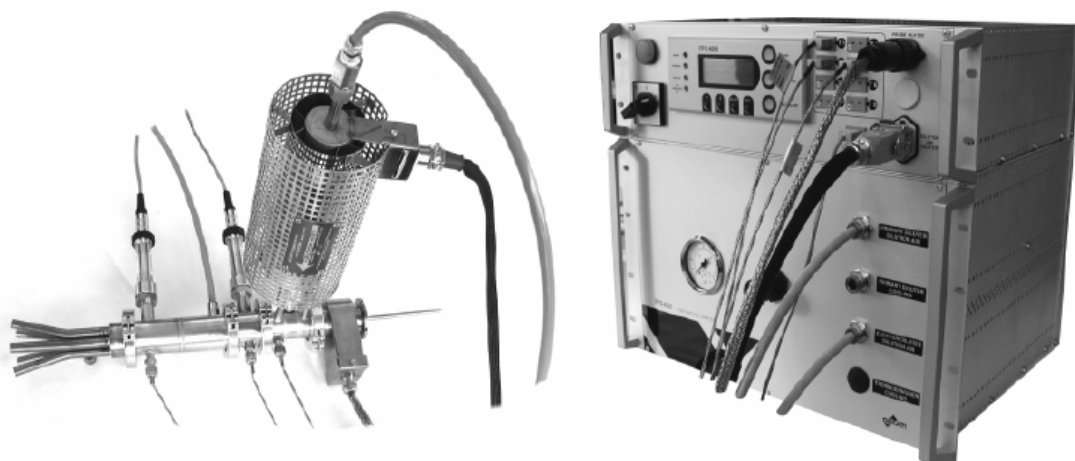


Figure A1: Fine Particle Sampler (FPS). From Dekati FPS manual.

Sample flows into the inner tube of the probe, while the dilution air is introduced through perforated walls. With this method, the flow of the dilution air through the entire length of the tube minimizes particle losses in the system. In addition, a distinct mode of nucleation may be created in desired cases. The dilution air flow is controlled using calibrated critical orifices inside the valve unit. The flow is directly proportional to the pressurized air pressure, which is continuously monitored. In addition, there are specially designed channels for cooling agent in the probe. Either water or air can be used for cooling. A temperature sensor is located inside the probe allowing continuous monitoring of the dilution point temperature. Location of the thermocouple is indicated in Figure A2.

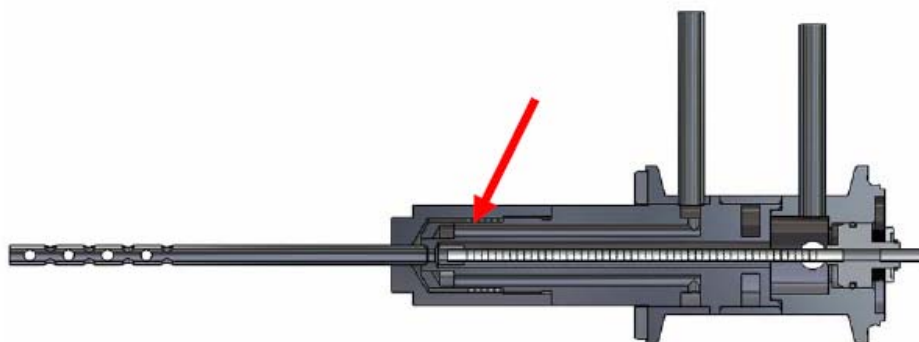


Figure A2: Schematic picture of the primary i.e. perforated tube diluter. The dilution air thermocouple position is indicated with an arrow. From Dekati FPS manual.

Ejector type diluter is used for secondary dilution (Figure A3). A controlled amount of secondary dilution air is conducted to a cavity outside the ejector nozzle. The nozzle is designed to cause a high velocity flow, which causes a pressure drop in the nozzle. Consequently, this pressure drop in the ejector nozzle sucks a flow from primary dilution.

Dilution ratio in this kind of construction is governed by four parameters: diluter dimensions, dilution air flow, sample temperature and the pressure drop in the ejector nozzle. The first parameter, ejector dimensions, controls the maximum pressure drop at the ejector nozzle. The flow pulled through the nozzle, i.e., from the primary diluter is proportional to the pressure drop. Due to this parameter, the units are calibrated individually. The second parameter, dilution air flow, is controlled using several critical orifices in the valve unit. The FPS software controls the magnetic valves inside the valve unit thus allowing different flow rates of dilution air into the diluter. Since the dilution ratio in this kind of ejector diluter depends also on the temperature and pressure difference between the inlet and the outlet, the temperature and pressure ratio are constantly monitored using a K-type thermocouple and two pressure sensors. The first pressure sensor is located upstream the ejector nozzle. The pressure fluctuations of the sampling point are damped by the primary diluter and the pressure is monitored continuously. The temperature sensor between the primary diluter and the ejector diluter is used for temperature compensations in dilution ratio calculation. As a result, continuous total dilution ratio can be calculated using the information from these signals. However, due to the ejector operation principle there are always some uncertainties in the dilution ratio calculation, e.g. cleanliness of the nozzle, pressure fluctuations etc. In order to maximize the accuracy of the measurement, it is always recommended to use a trace gas for precise dilution ratio measurement.

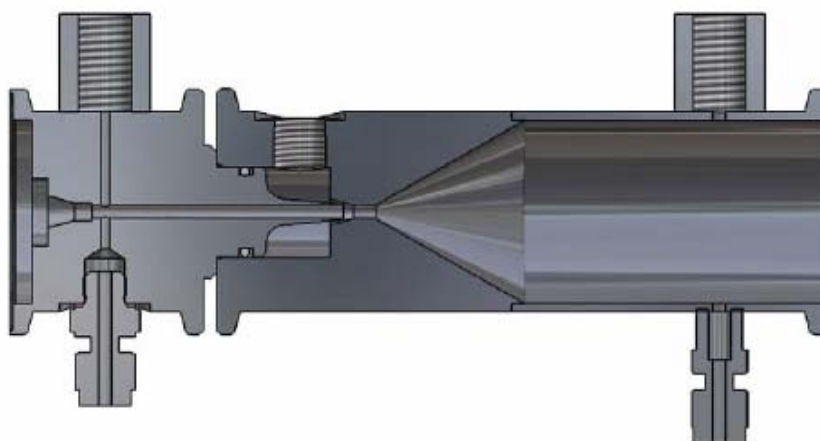


Figure A3: Schematic picture of the ejector diluter in the FPS. From Dekati FPS manual.

Typical sampling configurations

In this study most measurements were according to the PMP protocol (hot dilution). The dilution ratios used were between 25:1 and 40:1 (probe diluter dilution ratio 1.5:1 to 2:1 and ejector diluter dilution ratio 17:1 to 20:1). This factor was taken into account at the calculations. The temperature was set to **400°C** for the probe heater and **150°C** for the (ejector) dilution air in order to evaporate volatile particles and reduce the partial pressures of the gas phase species to prevent re-condensation at the diluter exit. These temperatures led to diluted aerosol temperatures at the exit of the diluter ~120°C.

The temperature of the evaporation tube (ET) was set at **400°C** in order to evaporate all volatiles and semi-volatile compounds. The residence time (RT) in this tube was estimated 0.15 s. Some measurements were conducted without any heating at FPS in order to measure volatile particles also (as nucleation mode or condensed material on the soot particles). These measurements are noted as “cold” dilution measurements because ambient temperature air was used for the dilution. The particles measured with cold dilution are called “wet” particles in order to distinguish them from the normal measurements (PMP protocol or “hot” dilution that give as a result non-volatile or “dry” particles). Immediately downstream of the evaporation tube there was an ejector diluter in order to minimize the diffusion losses, cool the hot diluted exhaust gas and reduce the particle number concentration below 10^5 cm^{-3} in order to be within the detection limit of the CPCs. The dilution ratio was constant **10.5:1** for the specific overpressure (1 bar) in this set up. An extra ejector diluter was used in some measurements (e.g. tailpipe and end anaconda) where the particle number concentrations were higher. The dilution ratio of this diluter was calculated **13.5:1**. The calculations of the dilution ratios were done with particle measurements upstream and downstream the diluters as no calibration gas or flow-meters were available at that period (xls file “**DRs for CVS modeling**”). The ejector diluters were cleaned only at the beginning of the measurement campaign. More details about FPS and ejector diluters can be found in the Annex 1.

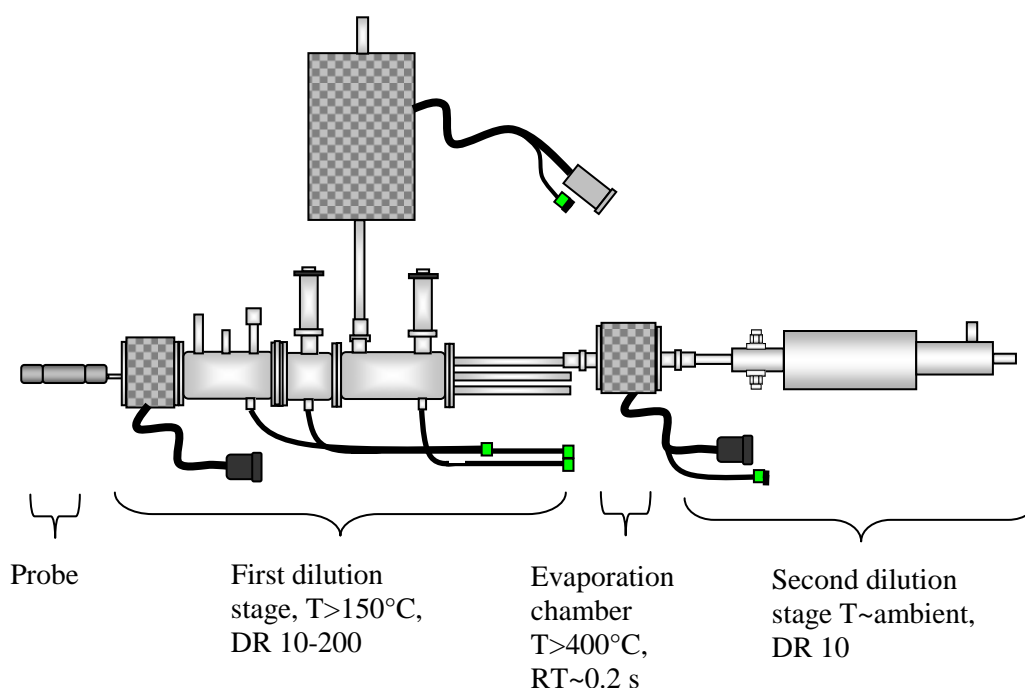


Figure A4: Set up during these measurements. From Dekati FPS manual.

B. DMM

Dekati Mass Monitor DMM-230 is a real-time device for automotive particulate mass emission measurements in the size range of 0 – 1.5 μm (Figure B1). The operation principle is based on particle charging, density measurement, particle size classification with inertial impaction, and electrical detection of charged particles (Figure B2). The device consists of a triode-type corona charger with on-line particle density measurement, and an inertial 6-stage impactor with electrical detection. A charger is used to give a known charge to particles. After charging region a static electrical field is used to deflect smallest particles to the charger mobility electrode; an electrometer is used to measure this current. A construction like this is used as a particle mobility size analyser. For the remaining particles the size classification is done in an inertial impactor that classifies the particles according to their aerodynamic properties. Sensitive electrometers are connected to impactor collection sensors and the measured current is proportional to the number of particles in corresponding size range. By combining the mobility and aerodynamic size information it is possible to calculate the effective density of the particles, and that information is used in conversion from measured current values to total particle mass. If the particle size distribution is bimodal or otherwise non-symmetric the mobility size determination is not possible, and therefore the density measurement cannot be used. Particle size distribution is monitored continuously, and if a bimodal distribution is detected the mass is calculated using unit density.



Figure B1: Dekati Mass Monitor (DMM). From Dekati DMM manual.

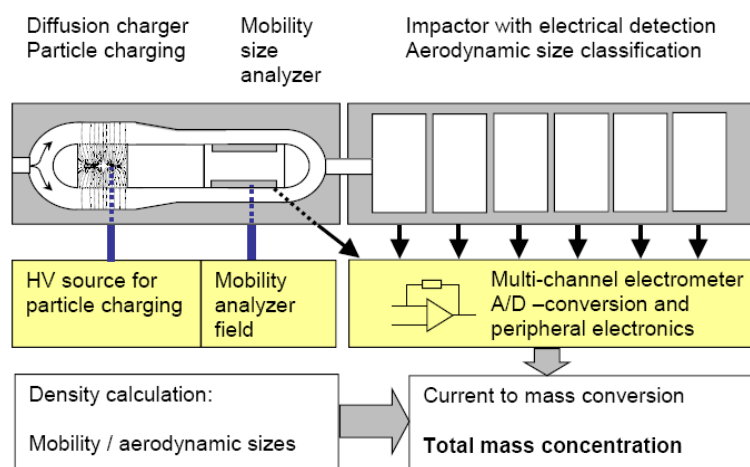


Figure B2: Principles of operation of DMM. From Dekati DMM manual

C. SMPS and CPCs

CPC 3010

The Model 3010 CPC, shown in Figure C1, is a compact, single particle counting instrument used in a variety of applications requiring detection of particles $0.01\ \mu\text{m}$ in diameter and larger. The Model 3010 CPC measures the number concentration of individual particles that are $0.01\ \mu\text{m}$ in diameter and larger. The particles are detected by condensing alcohol vapor onto the particles, causing them to grow into droplets (Figure C2). These particles, in droplet form, are easily counted by a simple optical particle detector. A heat sink, which makes up the entire back panel of the CPC, dissipates heat by natural convection. The cabinet purge airflow (1.0 lpm) helps to cool the electronics within the cabinet and creates a slight negative pressure within the instrument. Particles that may be generated inside the cabinet are quickly carried out through the vacuum line and do not contaminate the surrounding area.



Figure C1: TSI's CPC 3010. From TSI 3010 manual.

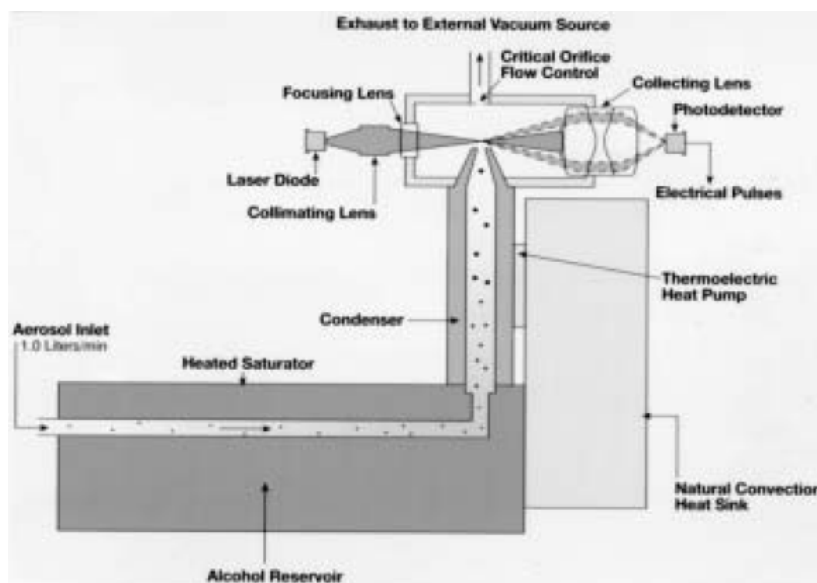


Figure C2: Theory of operation of CPC 3010. From TSI 3010 manual.

CPC 3025A (and DEKATI prototype)

The Model 3025A Ultrafine Condensation Particle Counter (Figure C3) uses a vapor sheath technique to improve the instrument's lower particle size sensitivity. This means that the counter is capable of measuring the number concentration of submicrometer airborne particles that are larger than 3 nanometers in diameter. The particles are detected and counted by a simple optical detector after a supersaturated vapor condenses onto the particles, causing them to grow into larger droplets. The range of particle concentration detection extends from less than 0.01 particle/cm³ to 9.99×10^4 particles/cm³. The UCPC uses a laser-diode light source; a condensing fluid; an internal microprocessor control; volumetric flow control; and a front-panel display of both particle concentration and instrument status; the instrument also offers the capability of full computer interfacing (Figure C4).



Figure C3: TSI's CPC 3025A. From TSI 3025A manual.

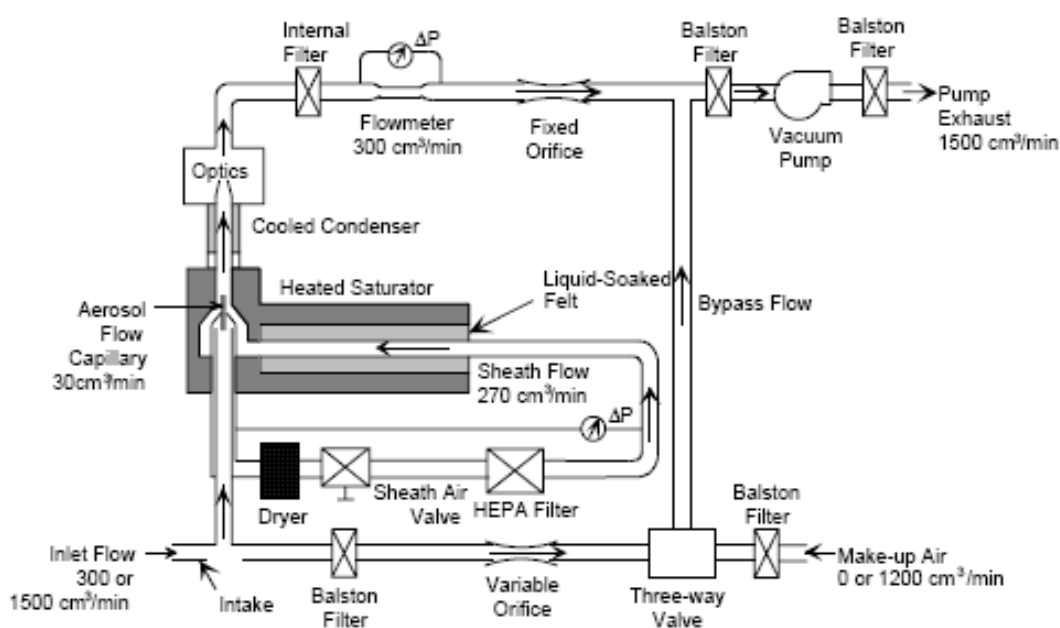


Figure C4: Flow schematic of CPC's 3025A. From TSI 3025A manual.

SMPS

The SMPS system is a system that measures the size distribution of aerosols in the size range from 5 nm to 1000 nm (Figure C5). Particles are classified with an Electrostatic Classifier and their concentration is measured with a Condensation Particle Counter (CPC). The SMPS system also uses a personal computer and custom software to control individual instruments and perform data reduction. The Model 3936 SMPS system measures the number size distribution of particles using an electrical mobility detection technique. The SMPS uses a bipolar charger in the Electrostatic Classifier to charge the particles to a known charge distribution. The particles are then classified according to their ability to traverse an electrical field, and counted with a Model 3010, (in these experiments) Condensation Particle Counter (CPC). The entire system is automated.

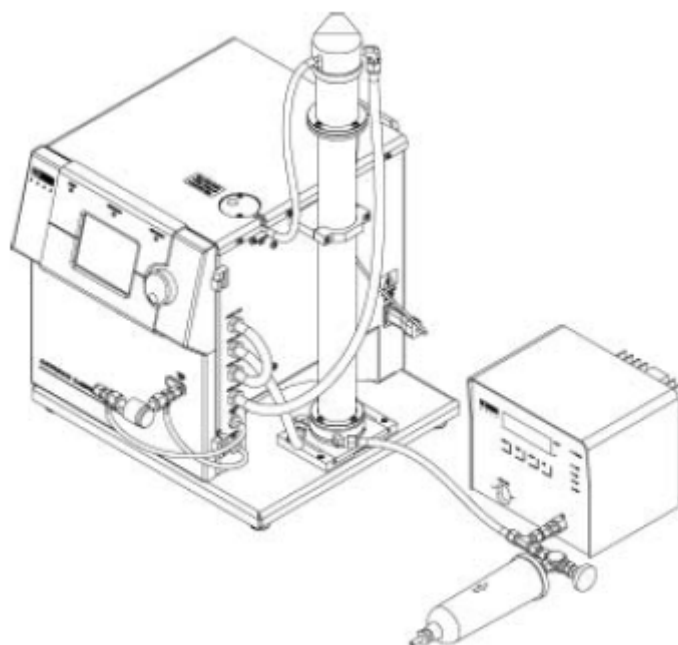


Figure C5: TSI's SMPS (Electrostatic classifier and CPC). From TSI SMPS 3936 manual.

In the Electrostatic Classifier, the aerosol enters a Kr-85 Bipolar Charger (or neutralizer), which exposes the aerosol particles to high concentrations of bipolar ions. The particles and ions undergo frequent collisions due to the random thermal motion of the ions. The particles quickly reach a state of equilibrium, in which the particles carry a bipolar charge distribution. The charged aerosol passes from the neutralizer into the main portion of the Differential Mobility Analyzer (DMA), shown in Figure C6. The DMA contains two concentric metal cylinders. The polydisperse aerosol and sheath air are introduced at the top of the Classifier and flow down the annular space between the cylinders. The aerosol surrounds the inner core of sheath air, and both flows pass down the annulus with no mixing of the two laminar streams. The inner cylinder, the collector rod, is maintained at a controlled negative voltage, while the outer cylinder is electrically grounded. This creates an electric field between the two cylinders. The electric field causes positively charged particles to be attracted through the sheath air to the negatively charged collector rod. Particles are precipitated along the length of the collector rod. The location of the precipitating particles depends on the particle electrical mobility, the Classifier flow rate, and the

Classifier geometry. Particles with a high electrical mobility are precipitated along the upper portion of the rod; particles with a low electrical mobility are collected on the lower portion of the rod. Particles within a narrow range of electrical mobility exit with the monodisperse air flow through a small slit located at the bottom of the collector rod. These particles are transferred to a particle sensor to determine the particle concentration. The remaining particles are removed from the Classifier via the excess air flow.

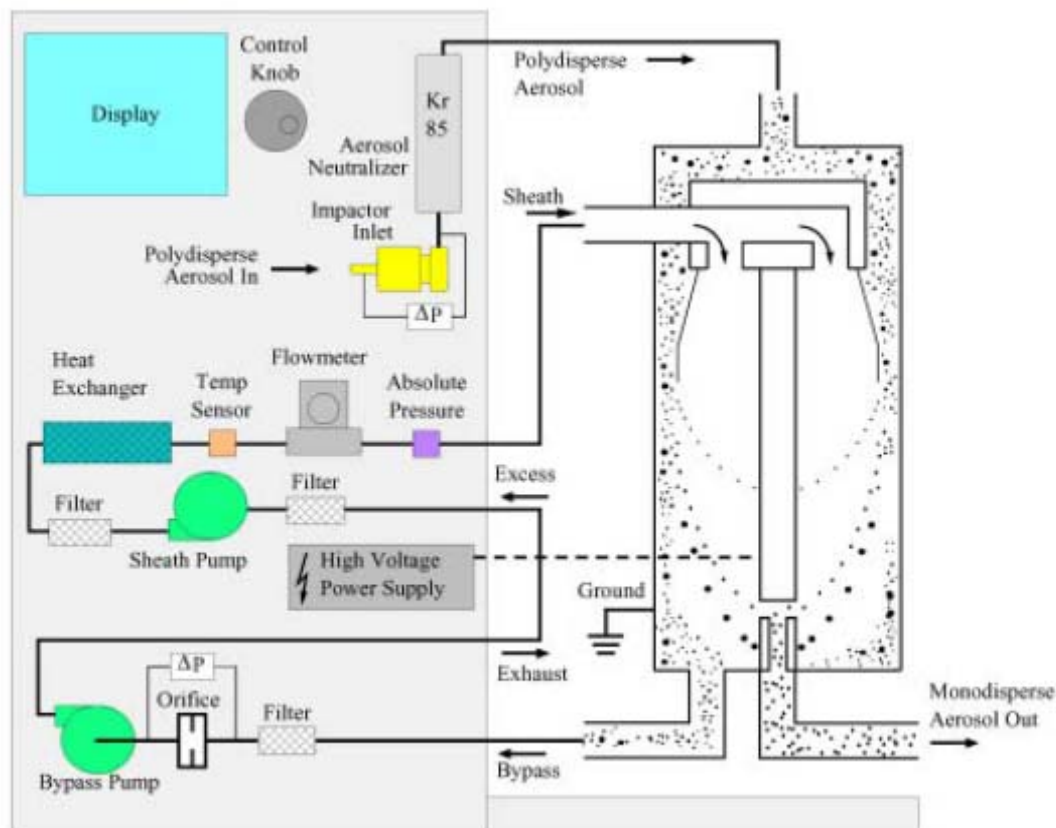


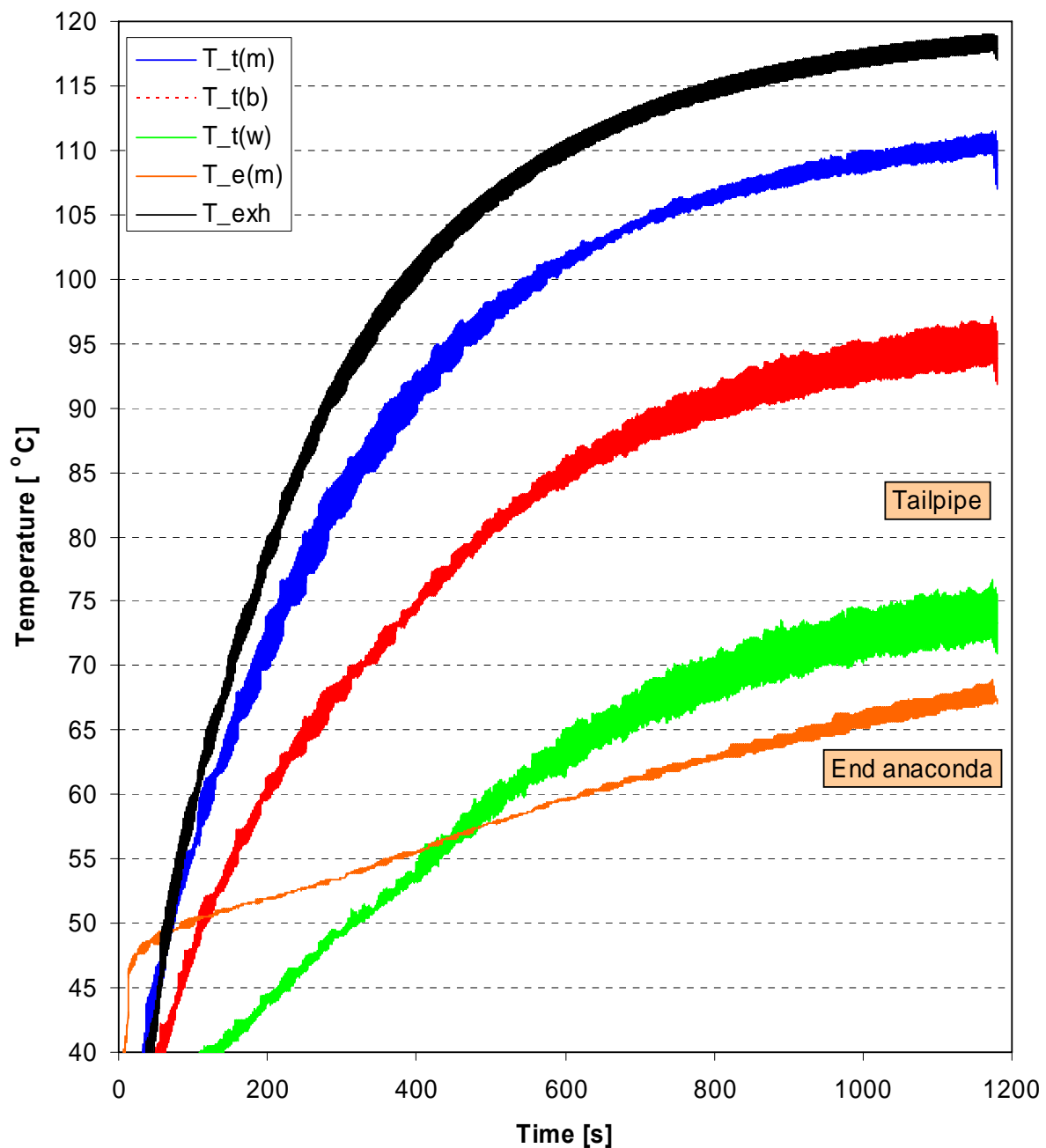
Figure C6: Flow Schematic for the Electrostatic Classifier with LDMA. From TSI 3936 manual.

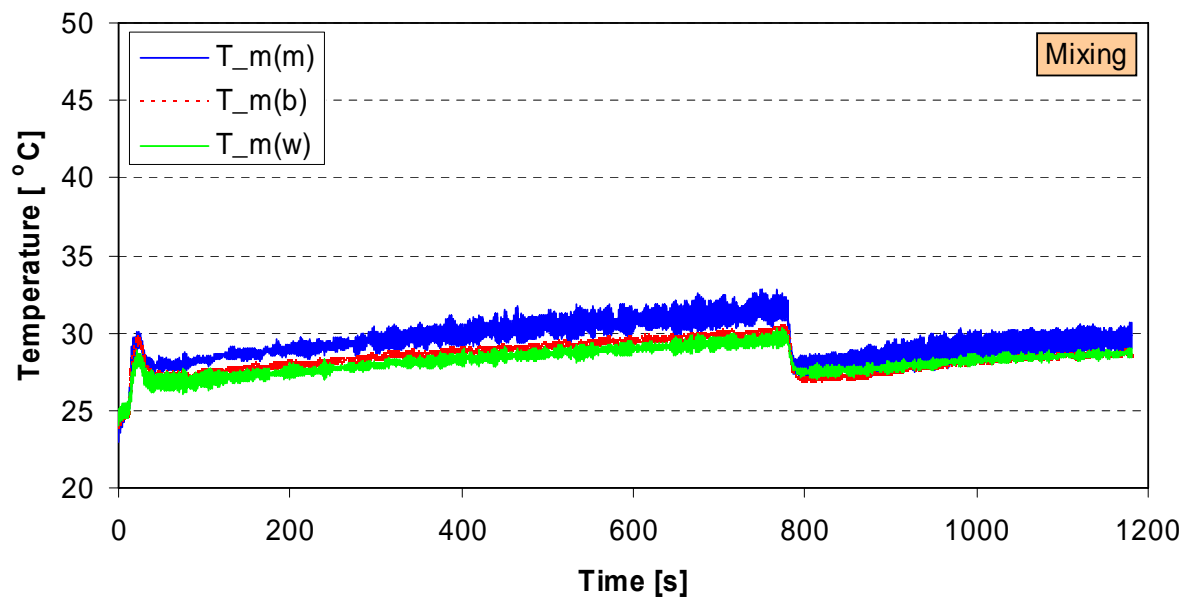
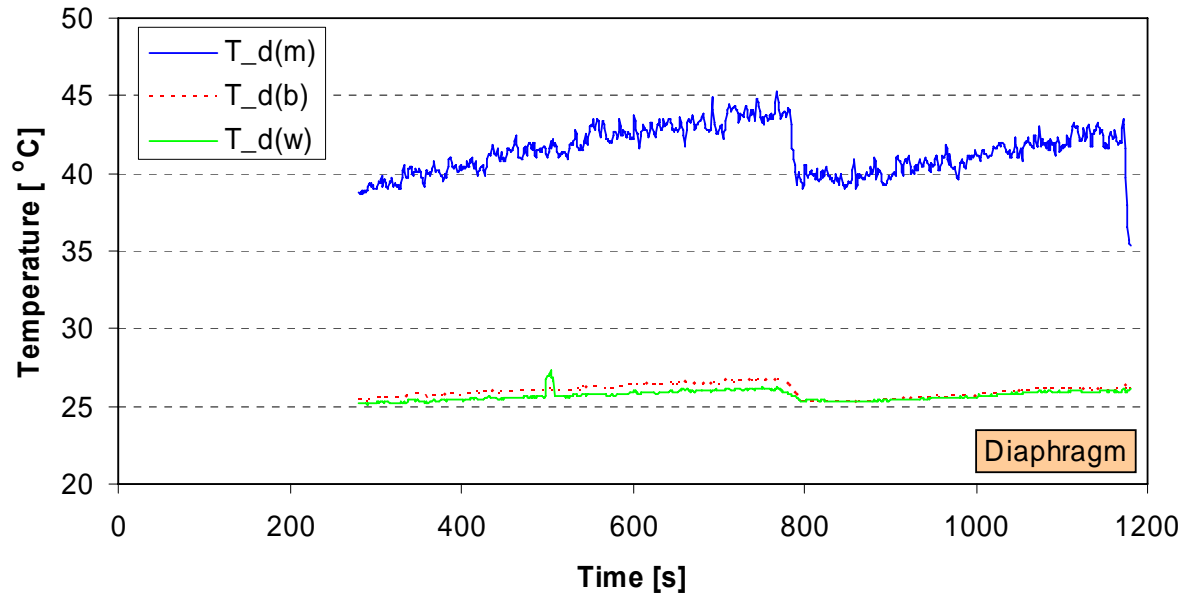
In this study sheath/sample flow rates used were 3/0.3 as it has been found that the 3936 neutralizer is not very efficient for higher flow rates. The flow rates were checked with a bubble flow-meter (BUCK calibrator M-5). The upscan and downscan times for the SMPS were 90/30 s respectively.

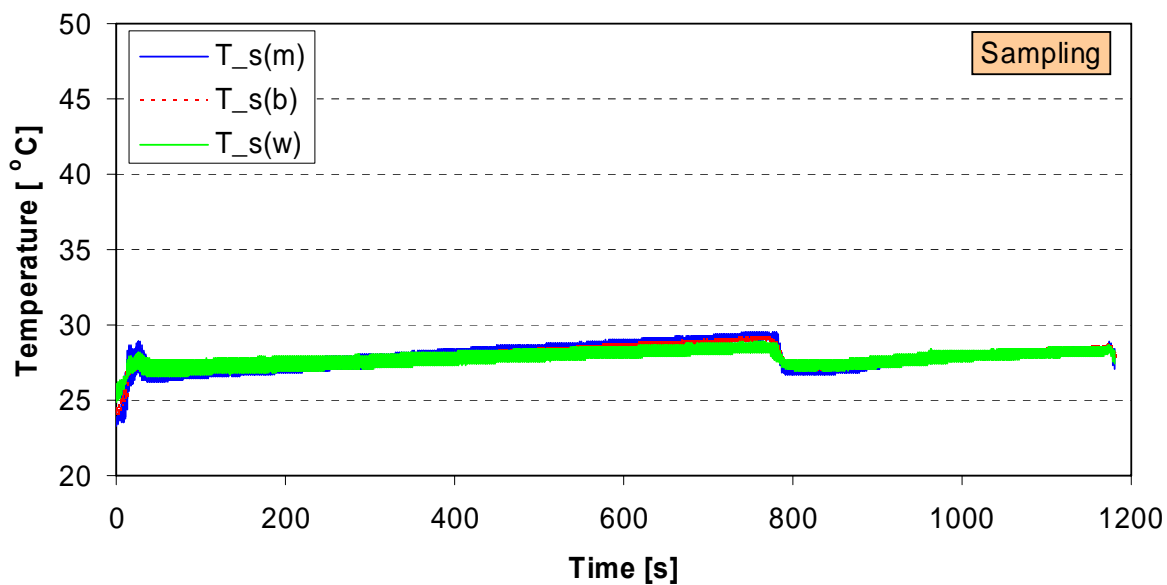
D. Temperature profiles at 50 km/h

The raw and averaged temperatures (T) are given in the xls file “TemperatureCVS” (available upon request). The second letter indicates the sampling position (Table 3) and the letter in parenthesis the position along the diameter (Table 4). Error bars show ± 1 standard deviation.

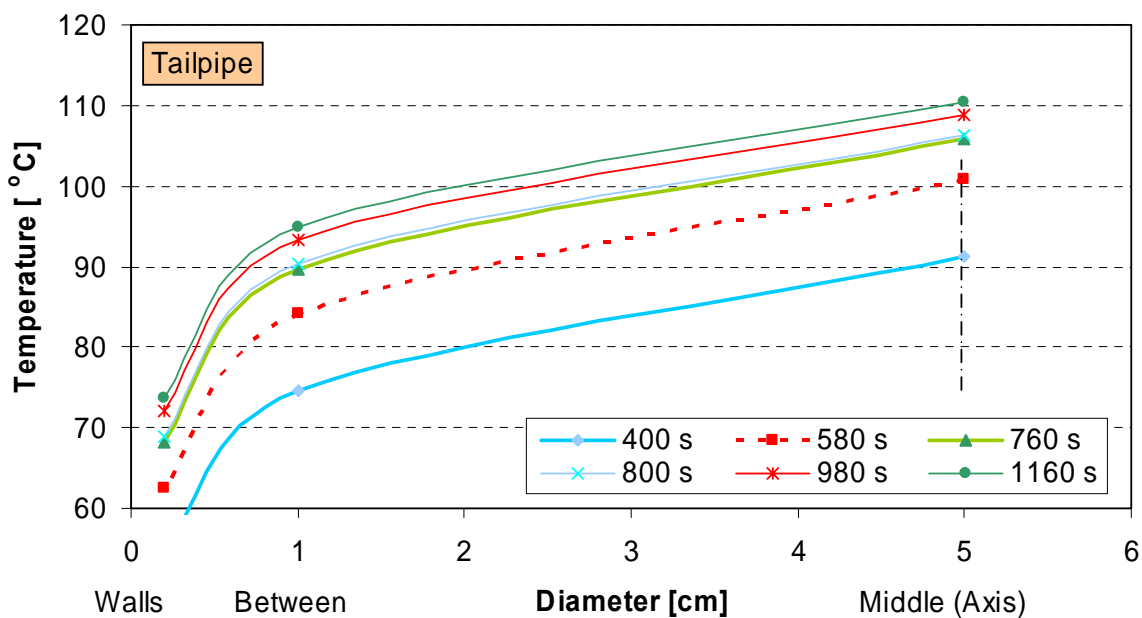
Temperature profiles over time

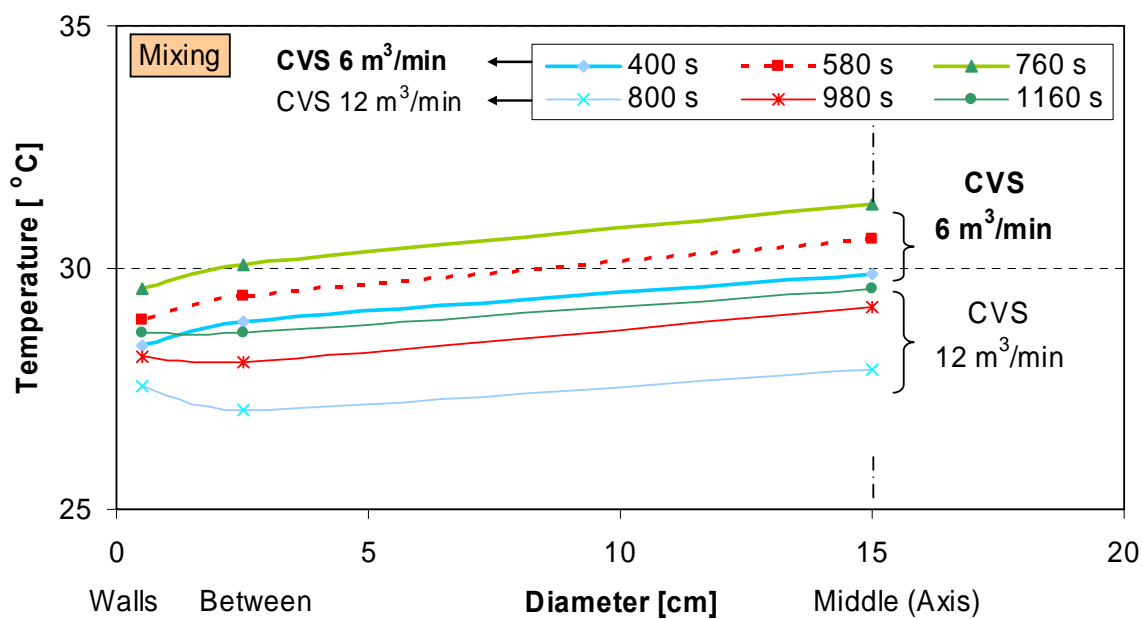
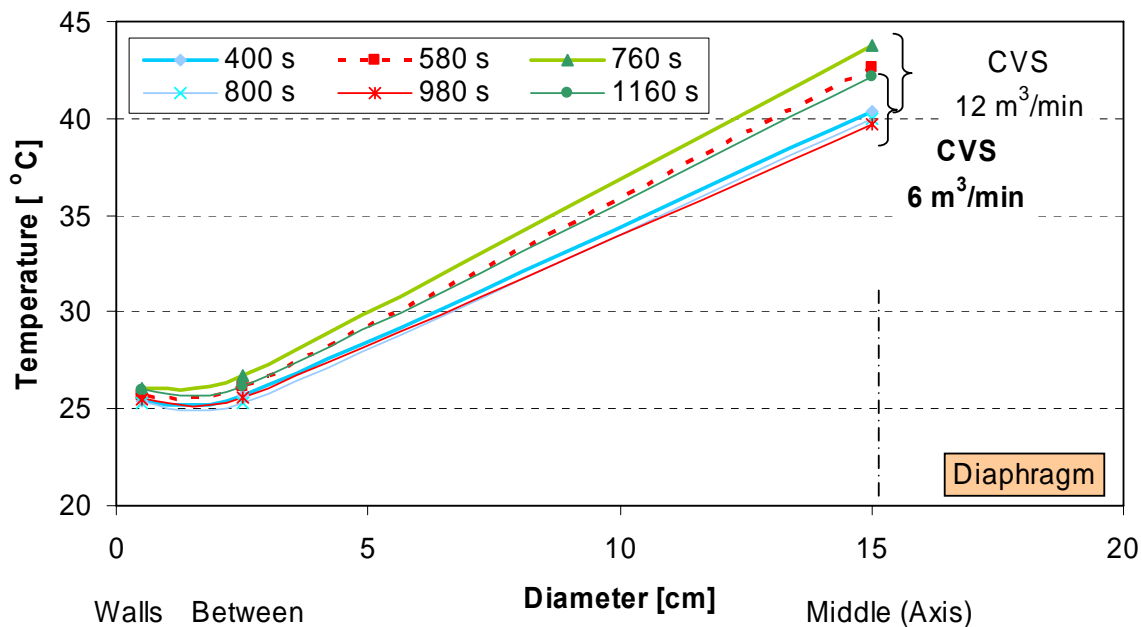


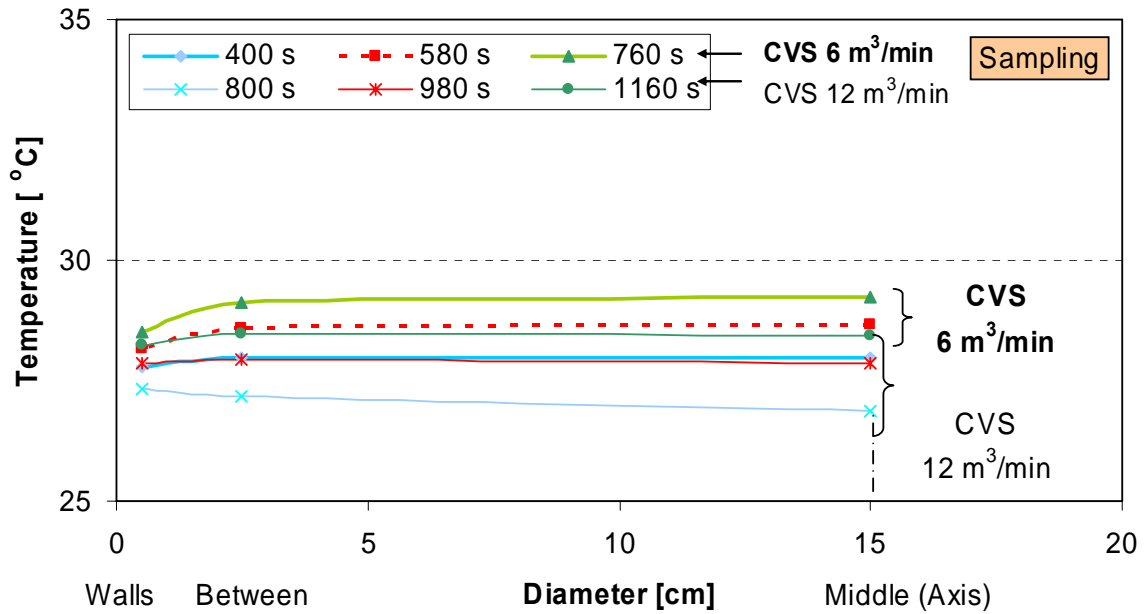




Radial temperature profiles



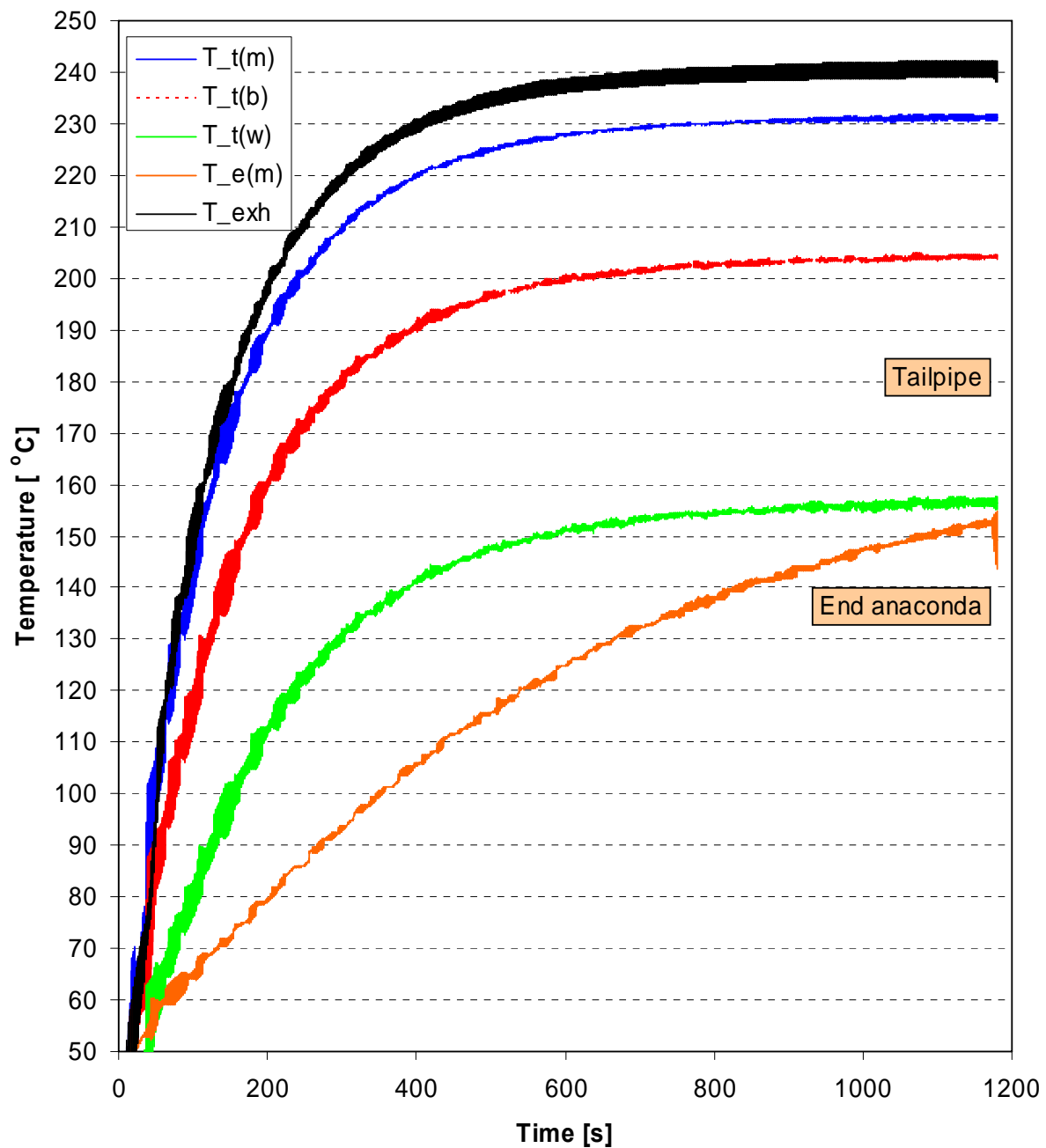


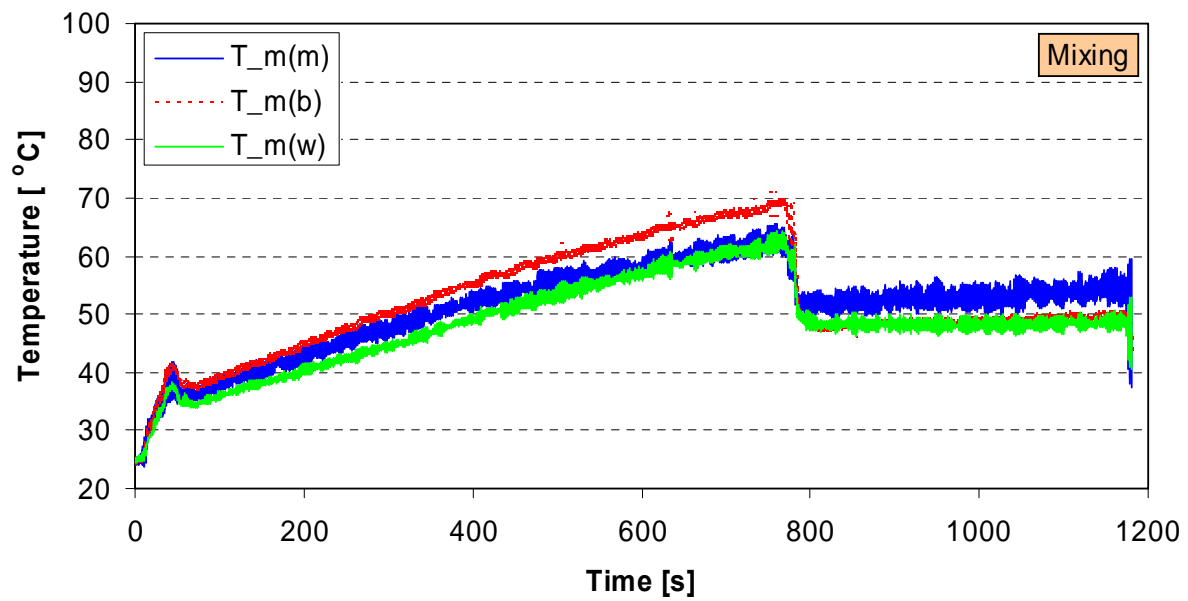
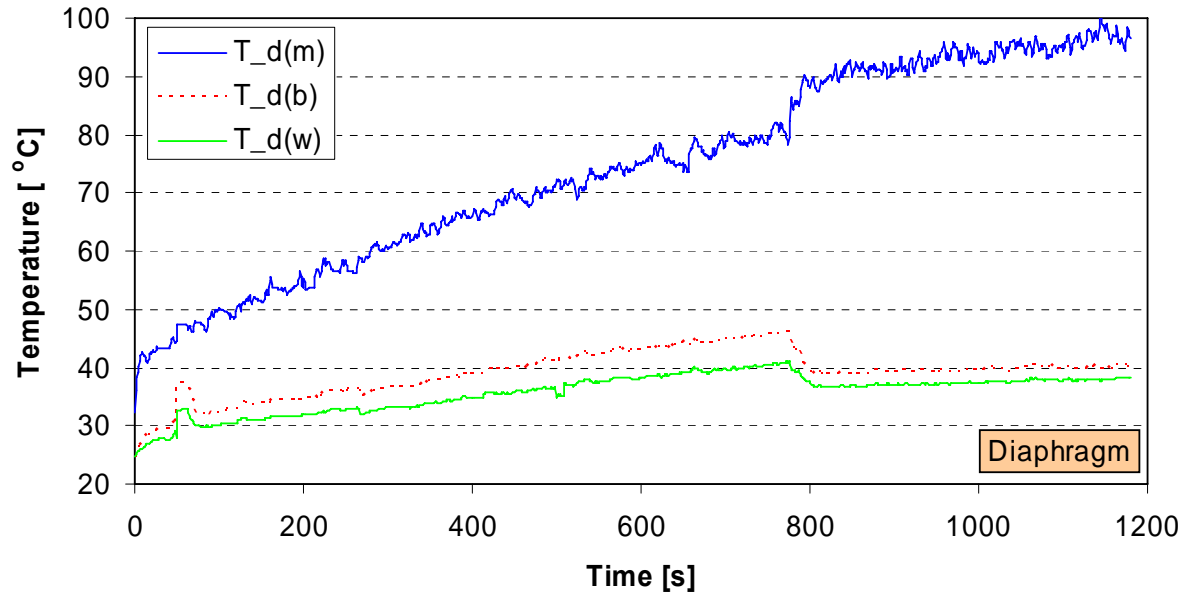


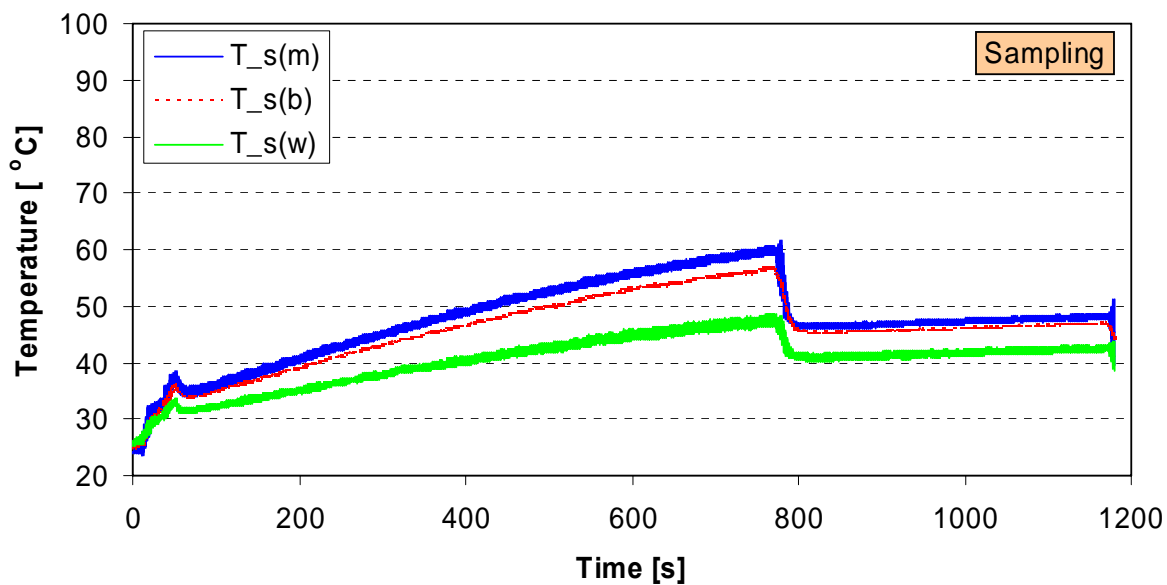
E. Temperature profiles at 120 km/h

The raw and averaged temperatures (T) are given in the xls file “TemperatureCVS”. The second letter indicates the sampling position (Table 3) and the letter in parenthesis the position along the diameter (Table 4). Error bars show ± 1 standard deviation.

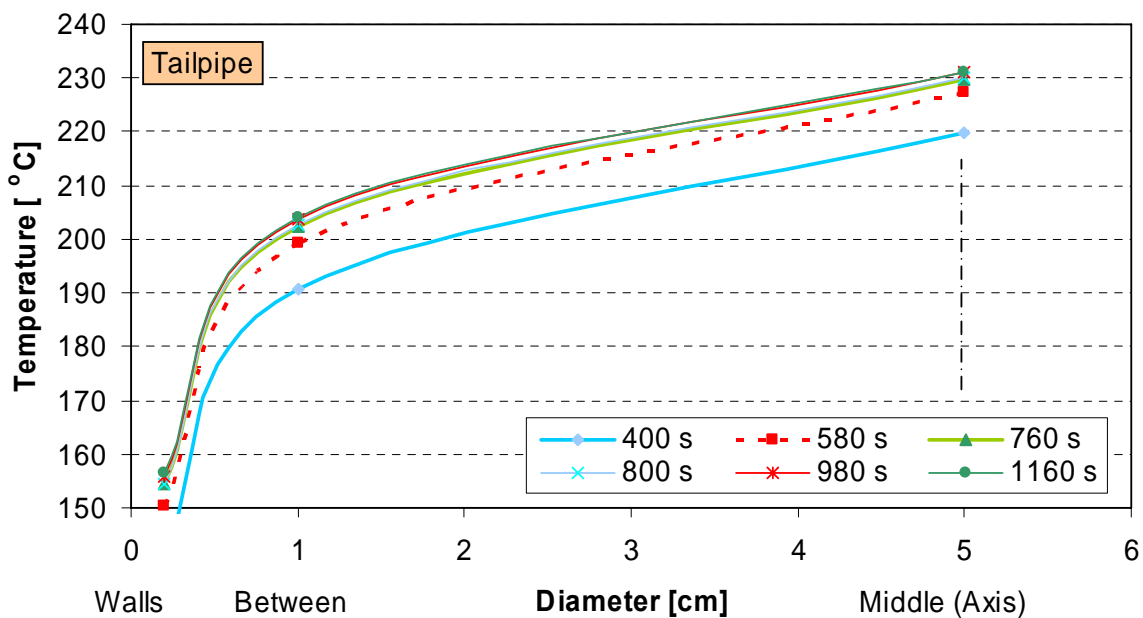
Temperature profiles over time

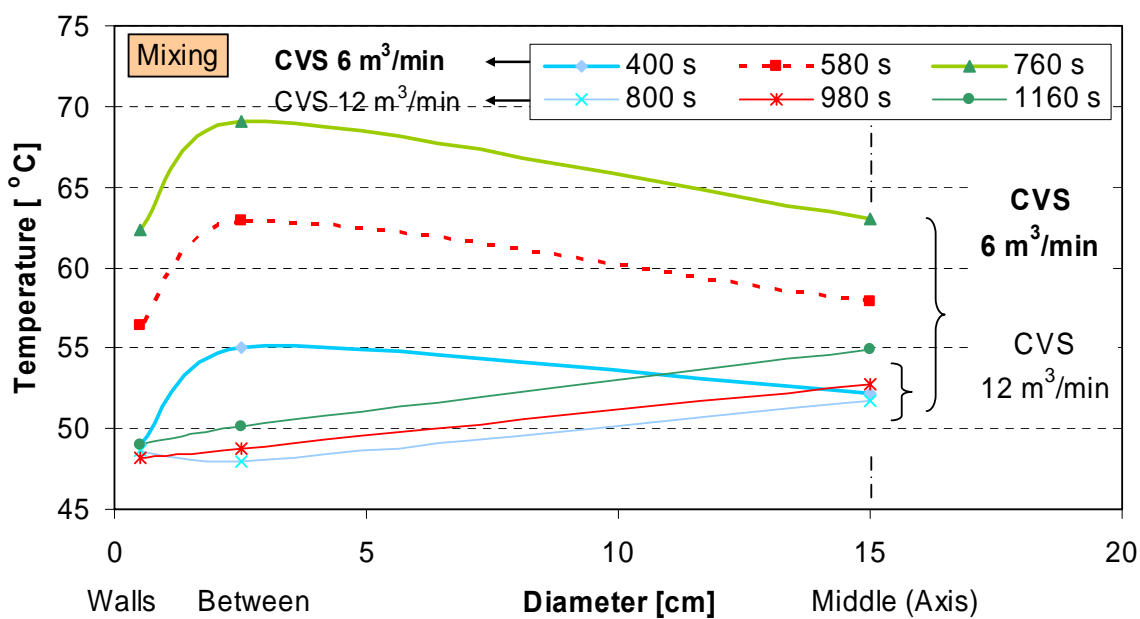
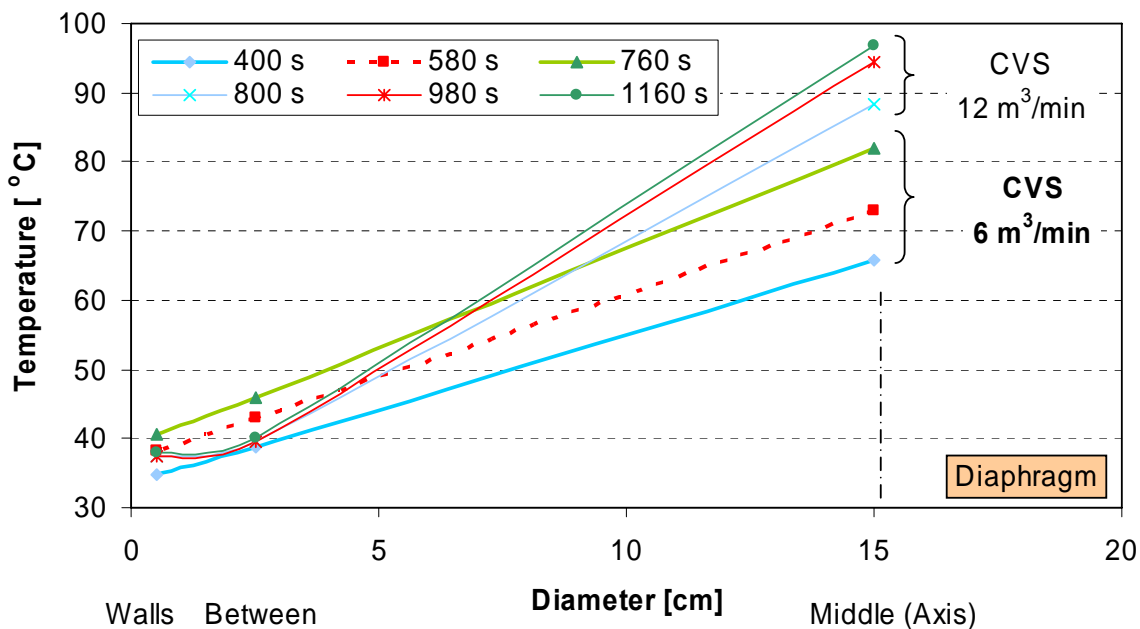


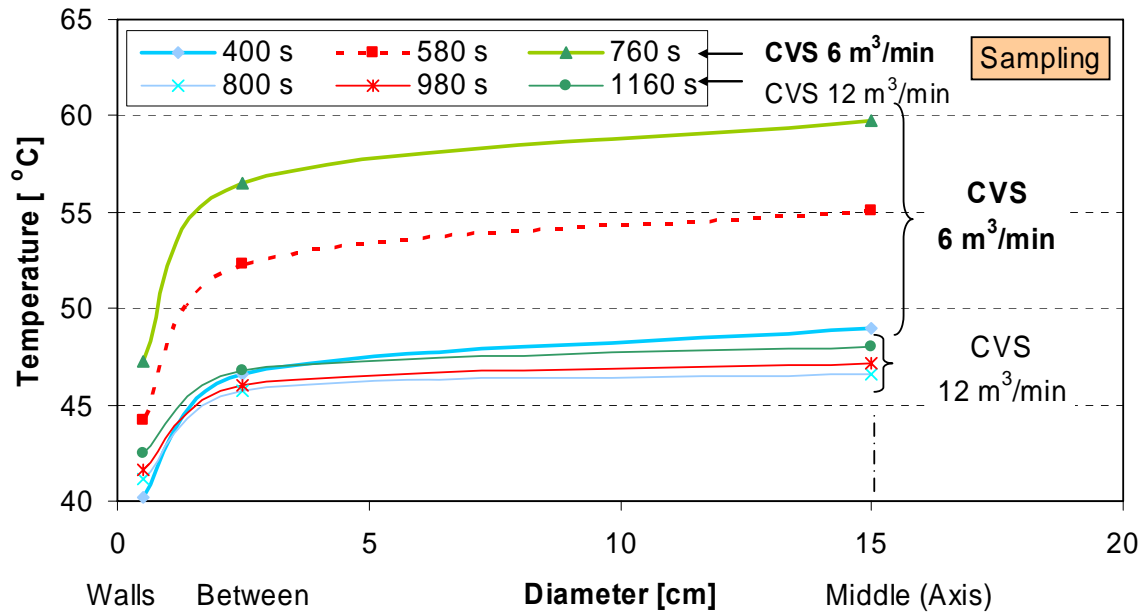




Radial temperature profiles







European Commission

EUR 23043 EN – Joint Research Centre – Institute for the Environment and Sustainability

Title: Measurements in support of modeling the VELA-2 experimental facilities

Authors: Barouch Giechaskiel, Lorenzo Isella, Rinaldo Colombo, Urbano Manfredi, Panagiota Dilara,

Yannis Drossinos, Alois Krasenbrink, Giovanni De Santi,

Luxembourg: Office for Official Publications of the European Communities

2007 – 50 pp. – 21 x 29.9 cm

EUR - Scientific and Technical Research series – ISSN 1018-5593

ISBN 978-92-79-07146-1

DOI 10.2788/55159

Abstract

This document reports the results of measurements conducted at the VELA-2 laboratories of the JRC in February 2007. The aim of the experimental campaign was to provide the necessary experimental data to model aerosol processes from the vehicle's exhaust tailpipe to the sampling point at the full dilution tunnel. The measurements included particle and temperature profiles at the tailpipe, at the end of the exhaust gas transfer tube to the dilution tunnel (anaconda), at the diaphragm of the dilution tunnel, 1,5 tunnel diameters downstream the diaphragm and 10 tunnel diameters downstream the diaphragm (normal sampling point). Two steady state speeds were used (50 and 120 km/h) and flow rates at the dilution tunnel of 6 and 12 m³/min. Non-volatile and total particle number and mass concentrations were measured according to the protocol of the Particulate Measurement Programme.

The results showed that the main changes of particle number distributions are observed along the transfer tube from the tailpipe to the dilution tunnel (anaconda). Afterwards the particle number distributions remain almost constant. However, low dilution at the dilution tunnel (flow rate of 6 m³/min) leads to a further small particle number distribution change.

How to obtain EU publications

Our priced publications are available from EU Bookshop (<http://bookshop.europa.eu>), where you can place an order with the sales agent of your choice.

The Publications Office has a worldwide network of sales agents. You can obtain their contact details by sending a fax to (352) 29 29-42758.

The mission of the JRC is to provide customer-driven scientific and technical support for the conception, development, implementation and monitoring of EU policies. As a service of the European Commission, the JRC functions as a reference centre of science and technology for the Union. Close to the policy-making process, it serves the common interest of the Member States, while being independent of special interests, whether private or national.

